

LAKE PANNON TRANSGRESSION ON THE WESTERNMOST TIP OF THE CARPATHIANS CONSTRAINED BY BIOSTRATIGRAPHY AND AUTHIGENIC $^{10}\text{Be}/^{9}\text{Be}$ DATING (CENTRAL EUROPE)

MICHAL ŠUJAN^{1*}, RÉGIS BRAUCHER², OLEG MANDIC³, KLEMENT FORDINÁL⁴, BIBIANA BRIKOVÁ⁵, RADOVAN KYŠKA PIPÍK⁶, VLADIMÍR ŠIMO⁶, MICHAL JAMRICH¹, SAMUEL RYBÁR¹, TOMÁŠ KLUČIAR^{1,7}, ASTER TEAM^{2**}, ANDREJ RUMAN¹, IVAN ZVARA⁵ & MICHAL KOVÁČ¹

¹Department of Geology and Paleontology, Faculty of Natural Sciences, Comenius University in Bratislava, Ilkovičova 6, 842 15 Bratislava, Slovakia. E-mail: michal.sujan@uniba.sk

²Aix-Marseille Univ., CNRS-IRD-INRAE-Collège de France, UM 34 CEREGE, Technopôle de l'Environnement Arbois-Méditerranée, BP80, 13545 Aix-en-Provence, France.

³Geological-Paleontological Department, Natural History Museum Vienna, Burggring 7, 1010 Wien, Austria.

⁴Dionýz Štúr Institute of Geology, Mlynská dolina 1, 817 04 Bratislava, Slovakia.

⁵Department of Applied and Environmental Geophysics, Faculty of Natural Sciences, Comenius University in Bratislava, Ilkovičova 6, 842 15 Bratislava, Slovakia.

⁶Earth-Science Institute, Slovak Academy of Sciences, Ďumbierska 1, 97401 Banská Bystrica, Slovakia.

⁷MM Revital, Šustekova 10, 851 04, Bratislava, Slovakia.

*Corresponding Author.

**Georges Aumaitre, Didier L. Bourlès, Karim Keddadouche

To cite this article: Šujan M., Braucher R., Mandic O., Fordinál K., Brixová B., Kyška Pipík R., Šimo V., Jamrich M., Rybár S., Klučiar T., Aster Team, Ruman A., Zvara I. & Kováč M. (2021) - Lake Pannon transgression on the westernmost tip of the Carpathians constrained by biostratigraphy and authigenic $^{10}\text{Be}/^{9}\text{Be}$ dating (Central Europe). *Riv. It. Paleontol. Strat.*, 127(3): 627-653.

Keywords: Late Miocene; Pannonian Basin System; facies analysis; shoal water delta; cosmogenic nuclide; paleogeography.

Abstract. The depocenters of epicontinental basins usually comprise relatively continuous depositional records, and these can be used in the determination of sediment routing and paleogeographic changes via a set of various geophysical, sedimentological, biostratigraphic and geochronological approaches. Although the margins of such basins will have a major role as constraints for that sediment routing, their depositional records are typically scarce and incomplete, posing a common challenge in terms of gaining information about them. The present study focuses on the upper Miocene succession present in the Malé Karpaty Mts., a pre-Cenozoic horst dividing the Vienna and Danube basins (Central Europe). The data gained by facies analysis, biostratigraphy, shallow seismic survey, authigenic $^{10}\text{Be}/^{9}\text{Be}$ dating and correlation of archival borehole profiles reveals, that the succession under consideration represents a record of the Lake Pannon transgression, which appeared in the study area at ~ 10.9 – 10.6 Ma. The subaerially exposed granitic massif and Middle Miocene successions sourced a shoal water delta, which intercalated with wave-induced dunes and open lacustrine muds in brackish sublittoral to marginal littoral environments. The granitic massif was probably also exposed later, during the regression of Lake Pannon at ~ 10.2 – 10.0 Ma, as a result of the progradation of the paleo-Danube delta from the Vienna Basin southeastwards. The depositional record of the regressive sequence was documented and dated in well-cores from the nearby Danube Basin margin. The documented scenario of transgression preceding the overall regression of the paleo-Danube delta system by a relatively short period is characteristic of several other localities across the Pannonian Basin System, and may imply that the progradation of depositional system caused a base-level rise on account of sediment loading-induced subsidence.

Received: October 14, 2020; accepted: July 16, 2021

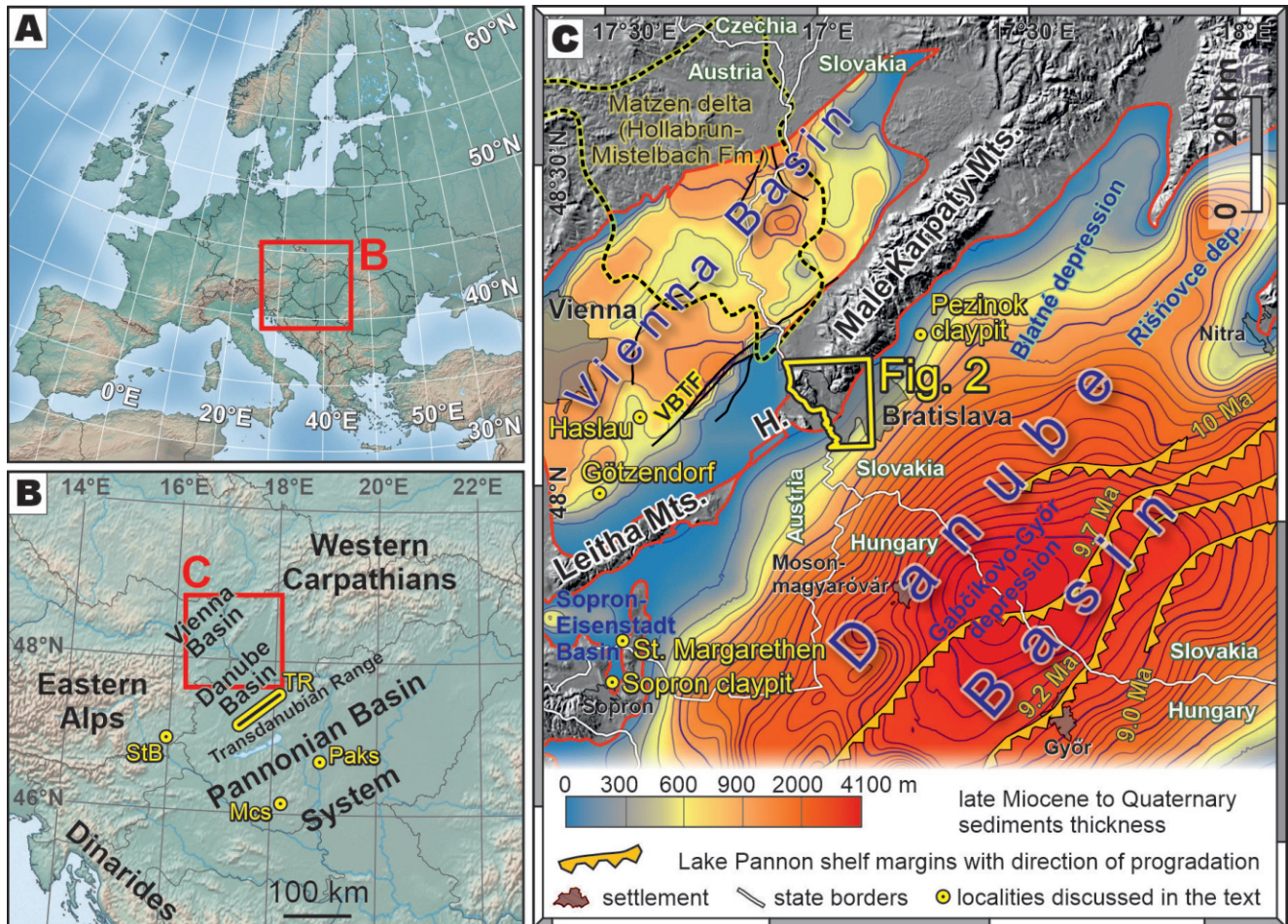


Fig. 1 - Location of the study area. A) General location within Europe. B) Location of the Malé Karpaty Mts. in the Alpine-Carpathian-Pannonian junction. Localities discussed in the Chapter 5.: StB – Styrian Basin, TR – Transdanubian Range, Paks – Paks boreholes, Mcs – Mecsek Mts. C) Location of the study area with thickness maps of the upper Miocene to Quaternary successions. Vienna Basin thickness map based on Berka et al. (2011) and Danube Basin thickness map according to Sztanó et al. (2016) and references therein. H. - Hainburg/Hundsheim Hills, VBTF – Vienna Basin transfer fault. Localities discussed in Chapter 5. are also depicted.

INTRODUCTION

Lake Pannon represents one of the most extensive long-lived brackish water bodies which appeared in Europe during the Neogene (Harzhauser & Mandic 2008; Magyar et al. 2013). The brackish water flooded a complex system of depocenters with water depth reaching 1,000 m as well as basement highs (Balázs et al. 2018). Although the paleobathymetry of basin floor environments is well constrained by seismic studies of shelf slope clinoform distribution (Uhrin & Sztanó 2012; Balázs et al. 2018), the determination of the extent of basin margins flooding is often difficult due to erosion, lack of seismic data and the coarse-grained nature of sediment, making the use of standard biostratigraphy of planktonic species difficult or impossible. However, the paleobathymetry of the margins of sub-basins

has played a major role in forming the pathways of depositional systems controlling the normal regression of Lake Pannon (Bartha et al. 2015; Sztanó et al. 2015). Hence, exploring the distribution of shallow lake facies can resolve the issue of paleogeographic changes, as well as the timing and intensity of tectonic events on the borders of a basin (e.g., Visnovitz et al. 2017; Harzhauser et al. 2018; Budai et al. 2019).

The present study is focused on the Malé Karpaty Mts., which divide the Danube and Vienna basins as the westernmost part of the Central Western Carpathians (Fig. 1). The question of the behavior of this mountain horst during the shift of the paleo-Danube delta from the Vienna Basin to the southeast during the early Late Miocene (~10 Ma) is still poorly understood and merits further investigation (Kováč et al. 2011; Šujan et al. 2016a; Joniak et al. 2020). The presence of an unspecified succession

of the Pannonian lacustrine sediments was detected during construction work and by geological mapping in the Mlynská dolina university campus in the city of Bratislava (Nemčok et al. 1966; Polák 2011). Hence, the deposits were excavated to study their facies and biostratigraphy, as well as to obtain numerical ages of deposition through the application of authigenic $^{10}\text{Be}/^9\text{Be}$ dating. In order to determine the position of the studied deposits within the Malé Karpaty Mts. clearly and to correlate them with equivalents in the neighboring basins, a shallow seismic survey was carried out, together with a study of archival borehole profiles. The goal of the study was to investigate the paleoenvironment and timing of the transgression of Lake Pannon in the study area. The resulting information sheds a new light on the evolution of the Malé Karpaty Mts. horst during the early Late Miocene and provides an important missing piece of the puzzle of paleogeographic changes in the early history of Lake Pannon.

GEOLOGICAL SETTINGS

The study area is located at the southwestern margin of the Malé Karpaty Mts., which divides the Neogene Vienna and Danube basins in Central Europe (Fig. 1). The Malé Karpaty Mts. and the Hainburg/Hundsheim Hills are considered the westernmost outcropping massif of the Western Carpathians (e.g., Hók et al. 2014). The horst in the study area is composed of crystalline rocks of the Tatric Unit of the Bratislava Massif (Fig. 2). These early Carboniferous granitoids form a part of the Alpine thick-skinned nappe, which is overthrust onto the Mesozoic sequence forming the northwestern part of the mountains and the basement of the Vienna Basin (Polák et al. 2012; Uher et al. 2014). The uplift of the Malé Karpaty Mts. started in the Early Pleistocene; it had very moderate and partly flooded relief during the late Pannonian/late Tortonian (Šujan et al. 2017; Šujan et al. 2018b; Joniak et al. 2020).

Both the Vienna and Danube basins were formed during the Miocene in, however, very different tectonic regimes. The lower Miocene fill of the Vienna Basin was accumulated in piggy-back depocenters above actively thrust Alpine napes. Major subsidence occurred under a pull-apart regime during the Middle Miocene, with the Vienna Basin transfer fault as one of the strike-slip fault systems open-

ing the basin (Fig. 1C) (Hölzel et al. 2008; Beidinger & Decker 2011; Lee & Wagreich 2017; Kováč et al. 2017). The basin experienced a less distinct subsidence phase during the early Late Miocene (Hölzel et al. 2008). The Middle Miocene (Badenian and Sarmatian) seas were replaced by Lake Pannon at the Middle/Late Miocene transition (~ 11.6 Ma) (Magyar et al. 1999; Harzhauser et al. 2003; Magyar et al. 2013). The lake formed a shallow water body with frequent water level oscillations related to deltaic progradation (Kováč et al. 1998; Harzhauser et al. 2004; Paulissen et al. 2011). The maximum extent of Lake Pannon in the Vienna Basin is estimated to have been at ~ 10.5 Ma (Harzhauser et al. 2003; Harzhauser & Mandic 2004). The final regression appeared between ~ 10.0 Ma and ~ 9.5 Ma and accumulation followed in alluvial settings at least up to ~ 8.0 Ma (Harzhauser et al. 2004; Paulissen & Luthi 2011). The Late Miocene (Pannonian) sequence reaches a thickness of up to ~ 1200 m and is overlaid discordantly by Quaternary alluvial and eolian deposits generally few tens of meters thick (Fig. 1C).

The Danube Basin comprises the northernmost depocentre of the Pannonian Basin System. Hence, it experienced the first maximum subsidence within the first syn-rift stage during the Middle Miocene (early Badenian), and this was related to the formation of a system of halfgraben depocenters (Tari et al. 1992; Horvath et al. 2006; Kováč et al. 2017; Balázs et al. 2017; Šujan et al. 2021). The early Late Miocene subsidence represents the last rifting phase, and is associated with normal faulting on the margins of depocenters and the accumulation of deep lacustrine, turbiditic, shelf slope to deltaic and alluvial facies in succession up to 4 km thick (Fig. 1C) (Tari 1994; Magyar et al. 2007; Kováč et al. 2011; Sztanó et al. 2016; Šujan et al. 2021). In contrast to the evolution of the Vienna Basin, the Danube Basin experienced intense accumulation during the basin inversion, resulting in a Pliocene to Quaternary alluvial sequence more than 800 m thick (Šujan et al. 2018b).

The late syn-rift tectonics, mostly expressed as normal faulting and the differentiation of the Lake Pannon bottom bathymetry (Balázs et al. 2018), probably resulted in the formation of archipelago-like low-relief horsts on the basin margins (Magyar et al. 2013; Budai et al. 2019). This was observed, for example, in the Transdanubian Range domain, where deltaic deposits directly overlie the pre-late Miocene rocks, and the remains of terrestrial mammal

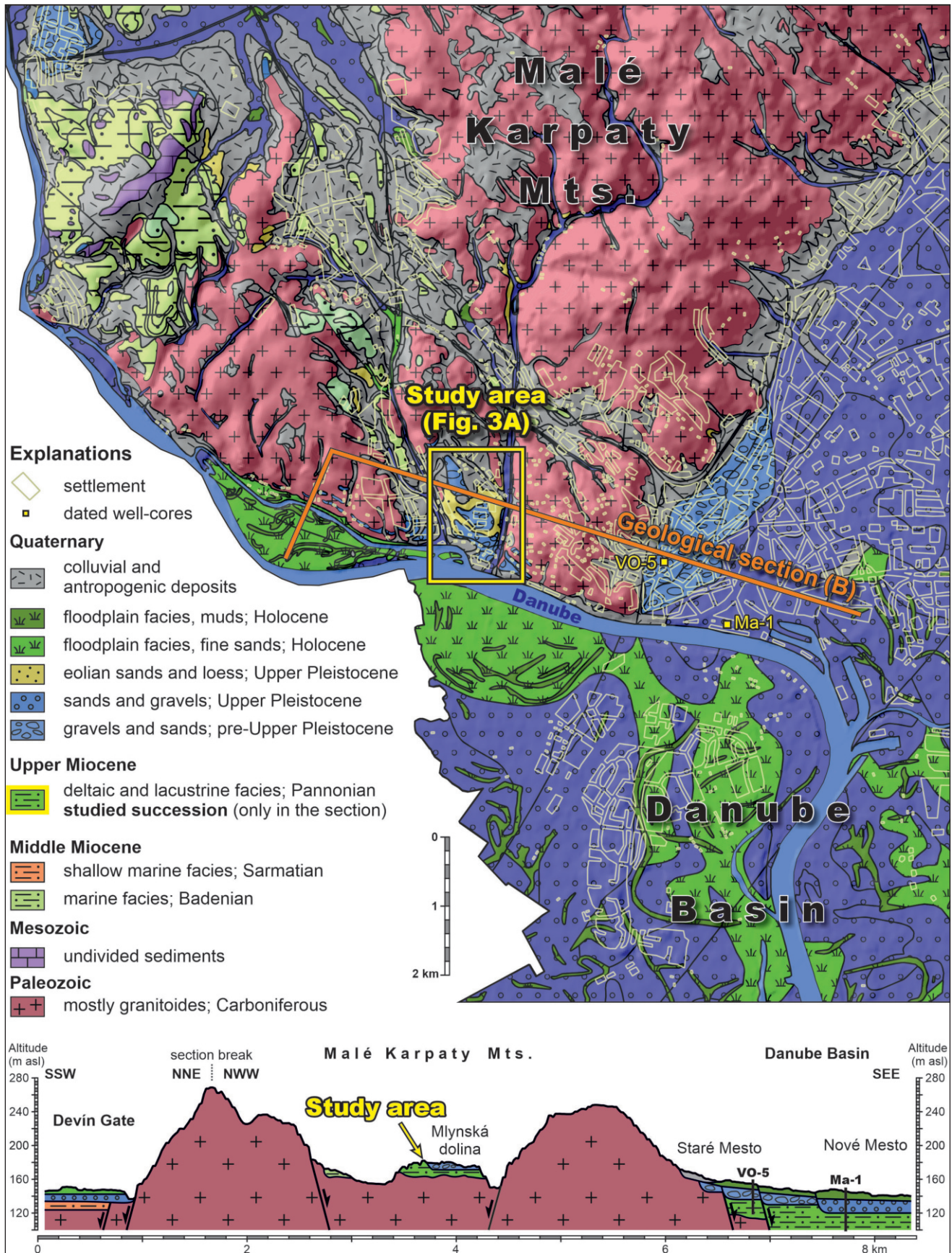


Fig. 2 - Geological map of the study area and generalized geological cross-section (modified from the Geological map of Slovakia 1:50,000). The Mlynská dolina, Staré Mesto and Nové Mesto represent districts of Bratislava. The Devín Gate is a tectonically predisposed valley occupied by the Danube flowing from the Vienna Basin towards the Danube Basin. The location of the imaged area may be found in Fig. 1. The complicated western margin of the map represents state borders with Austria.

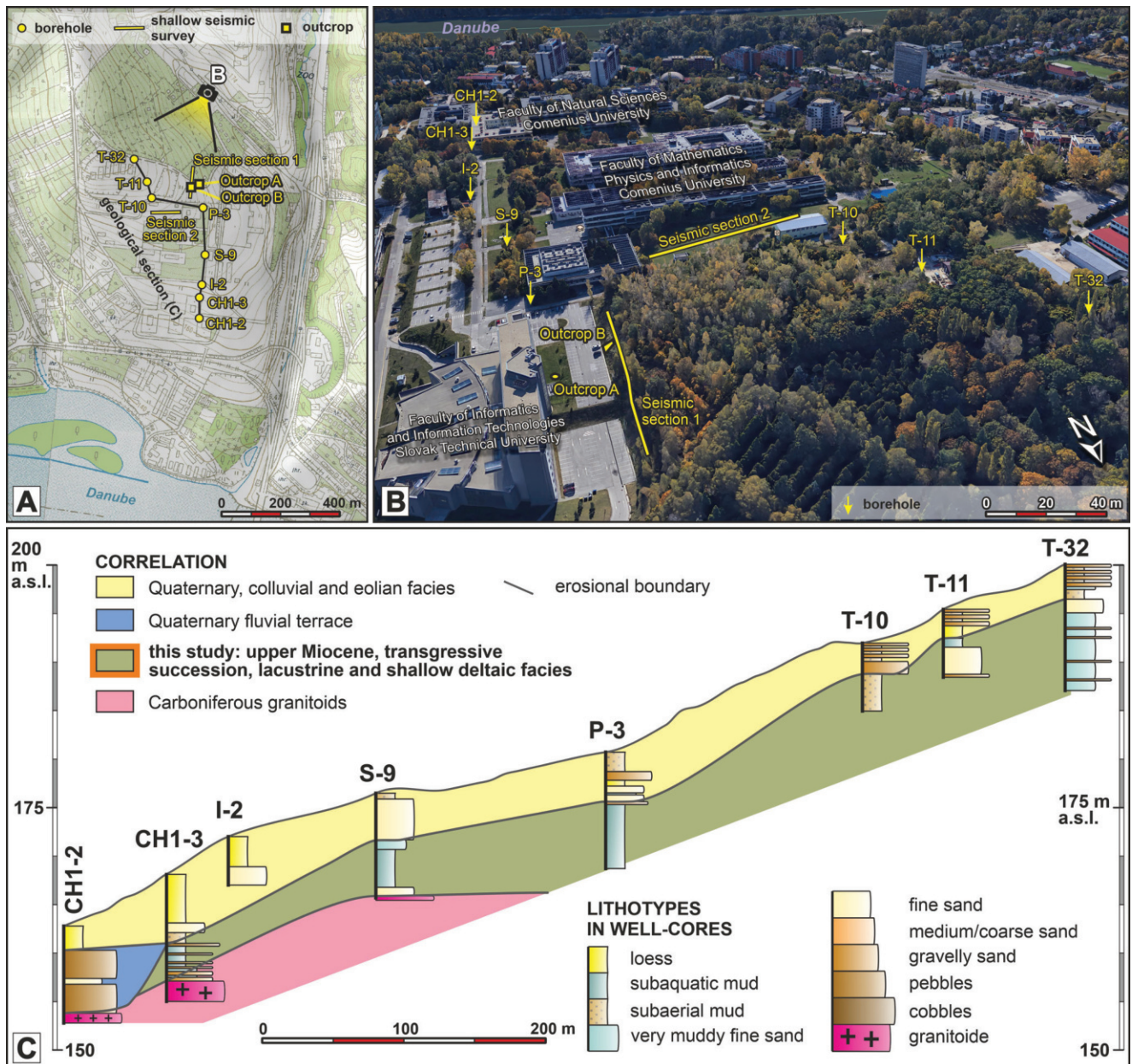


Fig. 3 - Location of the studied outcrops, archival boreholes and shallow seismic surveys. A) Topographic map. B) Panoramic view of the study area. C) Geological cross-section based on lithological logs of archival boreholes reinterpreted from Nemčok et al. (1966).

fauna of the Vallesian and Turolian ages (11.6–9.0 Ma and 9.0–5.3 Ma, respectively; Hilgen et al., 2012) were found in cavities (Meszaros 2000; Bartha et al. 2014; Bartha et al. 2015).

METHODS

Location of the excavation and archival well-core data

Since the study area is located within the urban area of Bratislava, several drillings had already been carried out at various sites in the past, mostly for engineering-geological purposes (Nemčok et al. 1966). The lithological description of these boreholes is available in the Geofond archive of the State Geological Institute of Dionýz Štúr, and was used to find suitable locations for the excavation of the upper Mio-

cene lacustrine sediments and for correlations. The sedimentological observations and sampling were carried out in two phases (Fig. 3): (1) a construction pit was opened during the year 2005, and an exposed outcrop (marked in this study “A”) served for biostratigraphic sampling for ostracods and general facies observations; (2) a new profile marked as “B” was positioned on a slope at a distance of ca. 33 m from the previous one, and which was subsequently excavated in 2016, since the original profile was already situated below the parking lot of the Faculty of Informatics and Information Technologies of the Slovak Technical University. The strata are in sub-horizontal arrangement and hence the stratigraphic (vertical) distance of the two profiles can be estimated, which comes to ca. 2 m. Outcrop B was examined for facies analysis, mollusk and nannoplankton biostratigraphy, and authigenic $^{10}\text{Be}/^9\text{Be}$ dating.

The correlation of the deposits studied in the vicinity of the outcrops, as well as towards the Danube Basin is based on lithological

logs of boreholes, which were obtained from the Geofond archive. The effectiveness of correlation of upper Miocene deposits in the Danube Basin relies on the lithostratigraphic concept applied. Previous correlations utilized archival borehole profiles, together with the original interpretation based on an earlier concept elaborated by Vass (2002), albeit with some modifications (e.g., Fordinál & Tuba 1992; Nagy et al. 1995; Fordinál & Harčová 1997). The upper Miocene lithostratigraphy was newly defined on the basis of genetic sedimentological criteria, considering all available geochronological data, by Sztanó et al. (2016), and the lithological well-core descriptions under consideration here were reinterpreted in terms of this concept. Besides the sedimentological criteria, which rely on an approach applied to correlative successions (Joniak et al. 2020; Šujan et al. 2020), also the original biostratigraphic data of mollusk and ostracod fossils were considered for purposes of facies associations determination in the logs.

Sedimentology

The facies were described in the standard way, on the basis of grain size, structure and texture, geometry and size of the strata and visualized in a sedimentological log (Stow 2005). Based on observed association of the facies, depositional processes were interpreted via the implementation of paleoecological data obtained from the fossil record. Special attention was paid to bioturbations (ichnofossils) within the section. More detailed observations were made and photo documentation carried out on new Outcrop B. Paleocurrent orientation measurement was possible using cross-stratification in the case of four beds.

Biostratigraphy and paleoecology

Mollusk specimens were collected during the excavation of Outcrop B and delivered to the Geological-Paleontological Department at the Natural History Museum (Vienna), where they were compared with the systematic bivalve collection and the relevant taxonomic literature (Hörnes 1862; Fuchs 1870; Schultz 2005).

Ostracods were sampled along the entire extent of Outcrop A in 2005, but they were present only in massive clay to silt. All samples taken were dried naturally in the laboratory, successively washed on a 0.09 mm sieve mesh, and picked up under a stereo-microscope in order to study the taxonomy, species composition and paleogeography of Ostracoda (Jiříček 1985; Meisch 2000).

Calcareous nannofossils were studied from 3 samples, designated FIIT 1, 2 and 3. Smear slides were prepared using the standard method (Bown 1998). Calcareous nannofossils were counted in 300 fields of view, using an Olympus BX 50 at 1250x magnification and oil immersion. An Olympus Infinity 2 camera, with QuickPHOTO CAMERA 2.3 software was used for the photography. The systematic identification of calcareous nannofossils was carried out using the taxonomy developed by Young (1998) and the MIKROTAX webpage established by Young et al. (2017). Standard nannofossil NN Zonation (Martini 1971) was used for age determination.

The original intention of studying foraminifera and palynomorphs from the three samples FIIT 1, 2 and 3 was not successful using standard methodology of preparation, since all samples were barren.

Authigenic $^{10}\text{Be}/^9\text{Be}$ dating

This method is based on the ratio of the radiogenic cosmogenic isotope ^{10}Be and stable ^9Be . Beryllium-10 is produced in the atmosphere by interaction with cosmic rays and transported to the hydrosphere by precipitation (Bourlès et al. 1989). ^9Be , in contrast, derives from the chemical weathering of rocks and the transport of the products of this process by runoff and streams. Both isotopes adsorb to the surface of clay minerals in the water column, and their ratio

changes in strict accordance with the decay of ^{10}Be (1.39 ± 0.01 Ma; Chmeleff et al. 2010; Korschinek et al. 2010), providing a chemically closed system. Since the source of the two isotopes is different, what causes variability in the initial ratio is the lithology of source rocks, depositional environment, denudation rate, geographical position and mixing of waters of various origins (Bourlès et al. 1989; Lebatard et al. 2008; Willenbring and von Blanckenburg 2010; Simon et al. 2016; Simon et al. 2020). Hence, the initial ratio of authigenic $^{10}\text{Be}/^9\text{Be}$ should be determined in order to provide an accurate calculation of the depositional age. Two initial ratios were determined for the Danube Basin for the dating of lacustrine and alluvial facies' depositional age (Šujan et al. 2016a); it was these which were employed by this study.

Five samples were analyzed, three originating from Outcrop B (FIIT 1, 2 and 3) and two sampled from the well-cores of boreholes on the Danube Basin margin (MA-1-153 and VO-5-51.8) (Fig. 2). The purpose of the latter two samples was to identify the age correlation between deposits on the mountain horst and the Danube Basin fill. However, only very small amount of material was preserved from the two cores and hence they proved adequate for only one dating sample each.

The samples were dried, crushed, and 1.5 g of material underwent leaching of the authigenic phase according to the procedure described by Bourlès et al. (1989) and Carcaillet et al. (2004), as modified by Šujan et al. (2018a) in the laboratory of the Department of Geology and Paleontology (Comenius University in Bratislava). Aliquots for AAS measurements of natural ^9Be concentrations were taken and 300 μl of the beryllium standard was then added. The following resin chemistry resulted in the separation of the beryllium from other elements (Merchel and Herpers 1999). Finally, BeO powder was oxidized in an oven, put in a copper cathode and the $^{10}\text{Be}/^9\text{Be}$ ratio was measured at ASTER, the French AMS national facility (Aix-en-Provence, France).

Shallow seismic survey

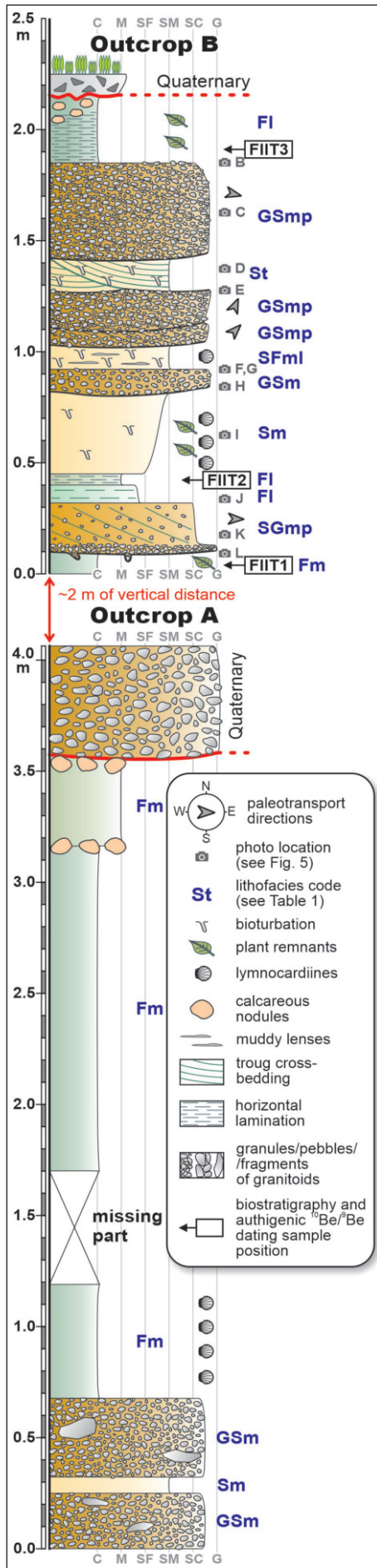
Seismic refraction tomography and reflection seismics were applied to determine the thickness and geometry of the upper Miocene deposits around the outcrop. The data were obtained using 24-channel DMT equipment with 10 Hz geophones, while 4 successive blows from a hammer served as the source of elastic waves. The distance between geophones was 5 m and points of elastic wave initiation were located in the middle of each pair of geophones, as well as 2.5 m before the first and 2.5 m after the last geophone. Two perpendicular profiles were measured, with the same length of 120 m. The model of seismic wave velocity distribution in the geological environment was produced by Reflexw Version 8.0 software (Sandmeier 2016).

The data thus obtained served as seismic refraction tomography models in a depth scale, and which were subsequently used for the determination of changes in seismic velocity in both vertical and horizontal directions. The seismic velocity information aided estimation of the depth scale in the case of seismic reflection profiles showing the geometry of the geological environment under consideration, although the resolution achievable using this method is lower than that attainable in seismic refraction tomography (Reynolds 1997; Sheehan et al. 2005).

RESULTS

Facies analysis

Description. The depositional record exhibits a heterolithic nature, with the alternation of sandy-gravelly and sandy units and mud-dominated units (Fig. 4). Description of all facies, their internal



fabric, geometry, trace fossil inventory and interpreted depositional processes are included in Table 1. Photo documentation of the facies may be seen in Figs. 5 and 6.

Interpretation. The sandy gravels or gravelly sands with faintly developed bedding (GSmp, SGmp; Fig. 5B–E, J–L) or with massive texture (GSm; Fig. 5F–H) are considered to be the result of surge-type deposition from small streams entering a relatively shallow lacustrine environment (Benvenuti 2003; Rossi et al. 2017). The lacustrine environment is implied by the simple horizontal burrows without walls produced by deposit-feeding ichnofauna (*Planolites*, *Thalassinoides*; Fig. 6A, B) (Tonkin 2012), present in the lowermost portions of the beds. The abrupt deposition and high flow concentration are likely to have caused the poor sorting (Cartigny et al. 2013), while modest rounding of the clastic material as well as its petrology implies very short transport. Comparable structures have been documented in shallow water deltas for example by Benvenuti (2003), Kostic et al. (2005) and Rohais et al. (2008). Some of the depositional events were preceded by erosion, forming the concave-upwards base of lens-shaped bodies (Fig. 5F, H).

The massive fine- to medium-grained sand contain frequent mollusks (Sm; Fig. 5I) and trace fossils of deposit-feeding ichnofauna (*Planolites*), as well as vertical dwelling burrows (*Skolithos* and *Ophiomorpha*; Fig. 5H), which may well have resulted from the opportunistic colonization of the sandy substrates following storms (Pemberton et al. 2012). The sandy lithology and moderate sorting imply deposition from currents despite the absence of primary structures, which is probably caused by bioturbation in a lacustrine setting. This lithofacies contain articulated shells of lymnocardines, implying their *in situ* appearance.

Fig. 4 - Sedimentological log of the studied outcrops. Lithofacies codes (blue) are described and interpreted in Table 1. Outcrop A: The excavation documented in 2005 for sedimentological observations and the biostratigraphy of ostracods. Outcrop B: The excavation documented and sampled in 2016 for facies analysis, authigenic $^{10}\text{Be}/^9\text{Be}$ dating and the biostratigraphy of mollusks and nannoplankton. Letters with a camera symbol indicate photographs in Fig. 5. Grain size codes: C - clay, M - mud, SF - fine-grained sand, SM - medium-grained sand, SC - coarse-grained sand, G - gravel.

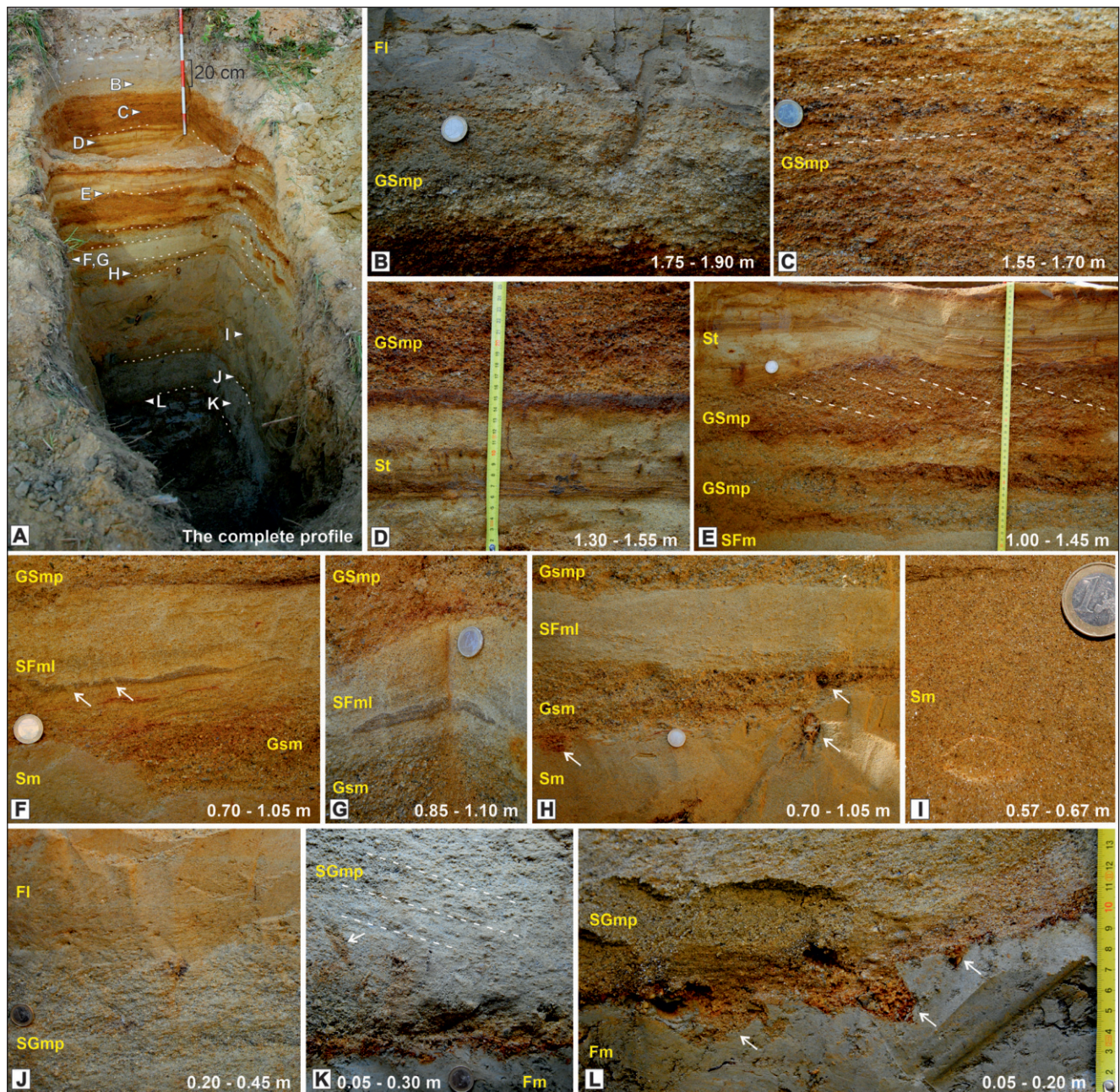


Fig. 5 - Documentation of facies. A) The complete excavation of Outcrop B performed by the authors in 2017 showing the positions of the detailed photos. B–L) Lithofacies are indicated by yellow symbols and discussed in the text and in Table 1. Trace fossils marked with white arrows: F - *Skolithos*; H - *Ophiomorpha*; K - aff. *Skolithos*; L – base of coarse sandy bed contains *Thalassinoides* burrows (arrows). The coin is 23 mm in diameter.

The origin of the Sm facies might be related to the joint appearance of massive to faintly laminated medium grained sand together of muddy lenses (SFml; Fig. 5F–H). The facies represent several events of sandy surge-type flows, separated by slow flows ($0.25\text{--}0.50\text{ m}\cdot\text{s}^{-1}$) or suspension deposition (Li et al. 2015; Yawar & Schieber 2017); this is also what is implied by the erosional nature of the upper boundaries of the muddy lenses. The deposition occurred in a lacustrine setting, close to a source of clastic sediment, as indicated also by the

association of trace fossils *Planolites* and *Skolithos* (Pemberton et al. 2012).

The trough cross-stratified medium grained sands with a thickness of $\sim 20\text{ cm}$ (St; Fig. 5E, Fig. 6C) show much better sorting. The low degree of bioturbation (*Planolites*, *Skolithos*, ?*Ophiomorpha*, ?*Arenicolites*) and good preservation of the texture indicate a dynamic environment with a sandy bed-load traction current. The nature of the beds and trace fossil association favor an interpretation of their origin as being from wave reworking of the

Tab. 1 - Lithofacies documented in the outcrops.

Code	Lithofacies description	Lithofacies geometry	Depositional process	Sedimentary environment
GSmp, SGmp, GSm	subangular to subrounded gravel containing granules, less pebbles, with high proportion of sand, or sand with high content of granules and less pebbles, massive (GSm) or with faintly developed planar cross-stratification (GSmp, SGmp), poorly to moderately sorted, clasts represent mostly fragments of granites, trace fossils <i>Planolites</i> and <i>Thalassinoides</i> on the base of a unit	sharp lower and upper boundary, base with complicated morphology indicating erosion, bodies forming lenses 10–50 cm thick	poor sorting and texture imply abrupt deposition from a surge-type laminar flow (possibly supercritical ?), single unit contain more depositional events due to bioturbation on its base	small stream delta front
Sm	massive fine- to medium-grained sand, moderately well sorted, with presence of articulated lymnocyprid shells, trace fossils <i>Planolites</i> , <i>Skolithos</i> and <i>Ophiomorpha</i> , plant detritus	tabular units 20–40 cm thick, transitional from fine grained facies, mostly with sharp erosive transition to gravelly facies	primary texture probably reworked by bioturbation, originally formed by traction current (?) according to the level of sorting	small stream delta-front subaqueous platform
SFml	massive to faintly laminated medium-grained sand with presence of bioturbations and lenses of mud, faintly developed horizontal lamination, moderately sorted, with presence of lymnocyprid shells, trace fossils <i>Planolites</i> and <i>Skolithos</i>	tabular units ~10 cm thick, sharp base, mostly with sharp erosive transition to gravelly facies	primary texture partly reworked by bioturbation, faint lamination and lenses of mud indicate several events of surge-type flow deposition separated by very slow traction currents or deposition from suspension	small stream delta-front subaqueous platform
St	trough cross-stratified medium-grained sand, moderately well sorted, with presence of trace fossils <i>Planolites</i> and <i>Skolithos</i> , questionable presence of trace fossils <i>Ophiomorpha</i> and <i>Arenicolites</i>	lenticular body with sharp concave upwards base and sharp upper boundary, ~20 cm thick	sandy bedload traction current induced by wave activity	3D dunes migrating on a small stream delta-front subaqueous platform
Fl	faintly laminated clay to silt, grey to greenish grey, frequent plant detritus, occasional presence of lymnocyprid shells	continuous horizontal bodies 5–50 cm thick, sharp lower and transitional upper boundaries	deposition from a slow traction current or from suspension	prodelta - subaqueous platform slope
Fm	massive clay to silt, grey, greenish grey to blue, appearance of plant detritus, occasional presence of lymnocyprid shells	horizontal bodies with relatively high thickness	deposition from suspension or slow traction currents, reworked by bioturbation	prodelta - subaqueous platform slope

material, supplied by the nearby small stream delta (Dumas & Arnott 2006; Pemberton et al. 2012; Vakarelov & Ainsworth 2013; Rossi et al. 2017).

The faintly laminated clay to silt deposits (Fl; Fig. 5B) have their origin in either slow traction currents ($<0.50 \text{ m}\cdot\text{s}^{-1}$) or from deposition from suspension. The lower degree of bioturbation compared to the massive muds (Fm) favor an origin in currents which might have induced stress on benthic fauna (Pemberton et al. 2012). The massive clay to silt (Fm; Fig. 5L, Fig. 6A, B) originated from a less dynamic environment, one which allowed ichnofauna to rework the original depositional texture (Pemberton et al. 2012). The two lithofacies were deposited close to a terrestrial source of sediment, as evidenced by the abundant plant remains.

Fossil assemblages

Trace fossils. Poorly preserved trace fossils were identified at the ichnogenus level. The simple vertical burrows with diameters of 3.5–7.0 mm without wall lining are attributed to *Skolithos* (Fig. 6C, D). Burrow depths are estimated up to the first 10 cm. *Skolithos* is interpreted as the dwelling structure of a wide variety of suspension-feeding organisms. *Skolithos*-dominated association occurs within the sequence of Sm, SFml, St lithofacies described herein. Vertical pairs of burrows reaching a diameter of 2–3 mm and with distance between parallel burrows ~5 mm were attributed with uncertainty to *Arenicolites* (Fig. 6D). However, no example of the typical U-shaped burrow of *Arenicolites* was found, though J-shaped burrows and parallel burrows were occasionally present. *Arenicolites* is

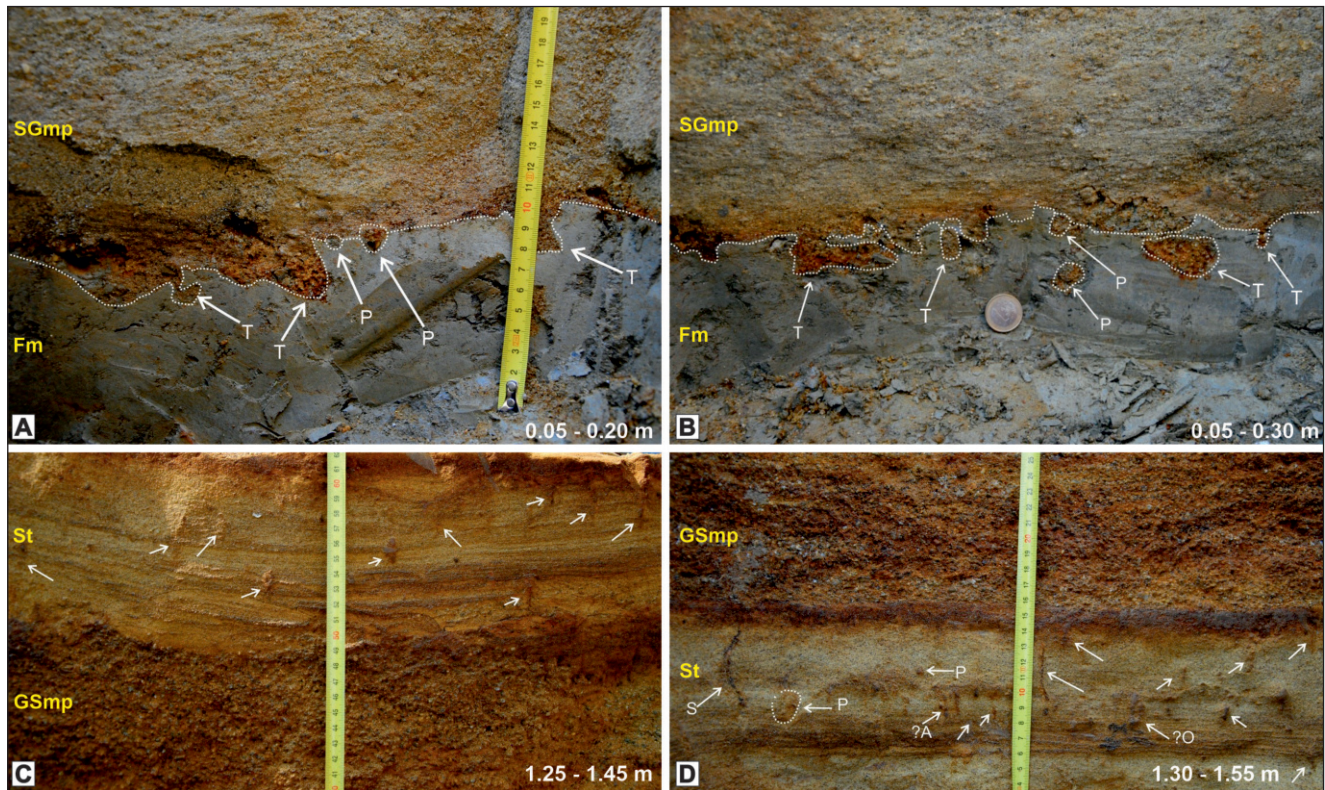


Fig. 6 - Documentation of trace fossils, indicated by white symbols and arrows. Yellow symbols are lithofacies codes (Table 1). A) Rounded trace fossils bounded by the lithological boundary represent ichnospecies *Planolites*; shapeless traces belong to *Thalassinoides*; B) Trace fossils bounded to the lithological boundary; P – *Planolites*, T – *Thalassinoides*; the diameter of the coin is 23 mm; C) monospecific association of *Skolithos* ichnogenera vertical burrows, low intensity of bioturbation; D) Vertical trace fossils dominate, S – *Skolithos*, P – *Planolites*, ?A – a sign of the U-shape indicate possible *Arenicolites* ichnogenera, ?O – a cross-section with a reddish wall resembles *Ophiomorpha*.

characterized as the dwelling burrow of a suspension-feeding organism.

Vertical/subvertical burrows with a wall diameter reaching ~26 mm are identified as *Ophiomorpha* (Fig. 5H). The depth of the burrows is estimated to be up to several tens of centimeters. Producers of *Ophiomorpha* are a wide range of shrimps of the families Callianassidae and Upogebiidae (Knaust 2012).

Perpendicularly cross-sectioned, horizontally oriented simple cylindrical burrows without walls were identified as *Planolites* (Fig. 6A, B, D). The diameter of the *Planolites* burrows ranges from 5 to 17 mm, and they are produced during deposit-feeding activity.

The largest burrows (with diameters from 12 mm up to 25 mm), which are without walls, but with branched horizontal tunnels and vertical shafts and coarse-grained passive infill are identified as *Thalassinoides* (Fig. 6A, B). The occurrence of trace fossils within coarse-grained lithofacies were strongly influenced by their low preservation potential. Trace

fossils with a high degree of contrast within coarse-grained and gravel lithofacies (*Thalassinoides*, *Planolites*) were distinguished only at the point of contact with muddy beds (Figs. 5L; 6A, B). *Thalassinoides* are the dwelling burrows of suspension and deposit feeding shrimps.

Mollusks. The fossil bivalves collected from Outcrop B are poorly preserved, despite their common presence as articulated specimens (Fig. 5I). In particular, they are present exclusively as internal casts due to post-depositional leaching of aragonitic shell material. Despite a careful comparison with the systematic bivalve collection of the Geological-Paleontological Department of the Natural History Museum, they cannot be identified with certainty at the species level. The morphology, however, reveals a genus level classification with *Lymnocardium* at a high level of certainty. The size, number of ribs, shell outline and convexity allow the tentative identification of specimens present (Fig. 7) as *Lymnocardium* cf. *conjungens* (Hörnes 1862) and *Lymnocardium* cf. *schedelianum* (Hörnes 1862).

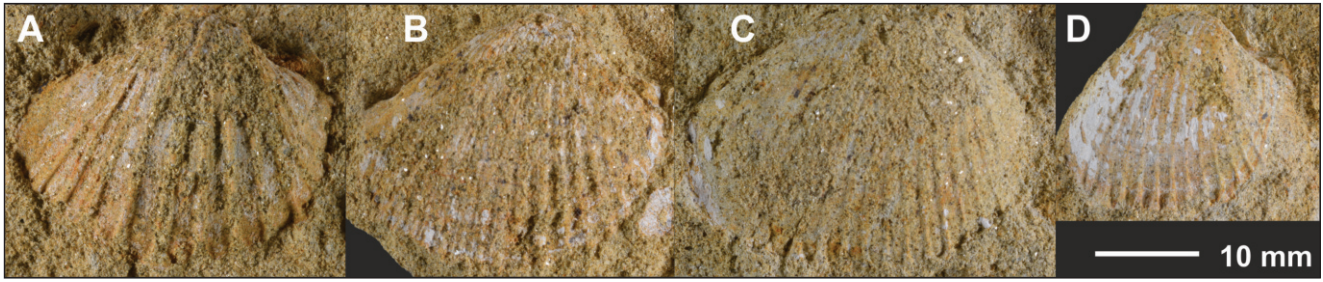


Fig. 7 - Mollusk specimens collected from Outcrop B. A) *Lymnocardium* cf. *schedelianum* (Hörnes 1862). B–D) *Lymnocardium* cf. *conjungens* (Hörnes 1862).

Ostracods. The association of ostracods is evaluated on the basis of all the samples taken from Outcrop A together, since the species' occurrence was stable along the section. The fossils collected are yellowish, opaque, chalky, seldom translucent, frequently broken and abraded. The species association comprises two different paleoecological groups (Fig. 8). The first group consists of fossil, Paratethyan endemic species characteristic of brackish limnic facies such as those appearing in the recent Caspian Sea: *Cyprideis* aff. *obesa* (Reuss 1850), *Cyprideis* sp., *Amplocypris abscissa* (Reuss 1850), *Herpetocyprilla auriculata* juv. (Reuss 1850), *Hemicytheria folliculosa* (Reuss 1850), *H. ex gr. omphalodes* (Reuss 1850), *Loxoconcha granifera* (Reuss 1850), *Lineocypris granulosa* (Zalányi 1959), *L. trapezoidea* (Zalányi 1929), *Lineocypris* sp., *Pontoniella* sp., *Xestoleberis* sp. On a generic level, the fauna is composed of the extant brackish *Cyprideis*, *Loxoconcha*, *Herpetocyprilla*, marine to brackish *Xestoleberis* and fossil Paratethyan genera *Amplocypris*, *Hemicytheria*, *Lineocypris*, and *Pontoniella*.

The second group represents freshwater species with morphological affinities to extant Holarctic fauna which live in variable freshwater biotopes

(Fig. 8): *Candona* sp. 1, *C. sp. 2*, *Candona ex gr. neglecta* Sars 1887, *Pseudocandona* sp., *Pseudocandona ex gr. eremita* (Vejdovský 1882), *Cyclocypris* sp.

Nannoplankton. Sample FIIT1 exhibited poor nannoplankton association comprising *Coccolithus pelagicus*, *Cyclicargolithus floridanus*, *Reticulofenestra minuta*, *R. pseudoumbilicus*, *R. haqii*, *Sphenolithus abies*, *Pontosphaera multipora*, ?*Discoaster adamanteus*, *Triquetrorhabdulus* sp., *Coccolithus formosus*, *Cyclicargolithus abisectus*, *Reticulofenestra bisecta*, *Broinsonia parca parca*, *Micula staurophora*, *Prediscosphaera cretacea*, *Retecapsa crenulata*, *Watznaueria barnesae* (Fig. 9, Table 2).

Sample FIIT2 may be considered poor in abundance of specimens with species including *Isolithus semenenko*, ?*I. pavelici*, *Reticulofenestra tegulata*, *C. floridanus*, *R. haqii*, *R. minuta*, *W. barnesae* (Fig. 9, Table 2).

Sample FIIT3 was barren of nanofossils and only clay minerals were observed.

Authigenic $^{10}\text{Be}/^9\text{Be}$ dating. The results of the beryllium isotopic measurements are summarized in Table 3. The degree of analytical uncertainty of $^{10}\text{Be}/^9\text{Be}$ ratio reaches relatively high values, ranging from 5.99% to 11.11%, increasing from sample FIIT1 to FIIT3, which probably mirrors their po-

Sample ID	Measured $^{10}\text{Be}/^9\text{Be} \times 10^{-14}$	^9Be (at.g $^{-1}$) $\times 10^{16}$	^{10}Be (at.g $^{-1}$) $\times 10^6$	Natural $^{10}\text{Be}/^9\text{Be} \times 10^{-11}$	Uncert. (%)	Age R_{0-L} (Ma)	Age R_{0-F} (Ma)	Mean weighted age R_{0-L} (Ma)	Mean weighted age R_{0-F} (Ma)
FIIT1	5.17	5.98 \pm 0.14	10.02 \pm 0.58	1.67 \pm 0.10	5.99	12.07 \pm 0.75	11.03 \pm 0.82	12.22 \pm 0.55	11.19 \pm 0.58
FIIT2	2.76	3.89 \pm 0.10	5.49 \pm 0.42	1.41 \pm 0.12	8.51	12.42 \pm 1.02	11.37 \pm 1.04		
FIIT3	3.52	4.85 \pm 0.17	7.00 \pm 0.73	1.44 \pm 0.16	11.11	12.37 \pm 1.36	11.32 \pm 1.33		
MA-1-153	3.07	2.85 \pm 0.16	6.14 \pm 0.44	2.15 \pm 0.20	9.30	11.57 \pm 1.06	10.52 \pm 1.06	11.32 \pm 0.73	10.27 \pm 0.73
VO-5-51.8	9.62	7.08 \pm 0.13	19.41 \pm 1.71	2.74 \pm 0.25	9.12	11.09 \pm 1.00	10.04 \pm 1.00		

Tab. 3 - Authigenic $^{10}\text{Be}/^9\text{Be}$ isotopic data from outcrop B and from well-cores Ma-1 and VO-5. The ages were calculated separately using lacustrine (R_{0-L}) and floodplain (R_{0-F}) initial ratios according to Šujan et al. (2016a): $R_{0-L} = (6.97 \pm 0.14) \times 10^{-9}$, $R_{0-F} = (4.14 \pm 0.17) \times 10^{-9}$. Processing a blank sample resulted in an AMS $^{10}\text{Be}/^9\text{Be}$ ratio of 1.11×10^{-14} . Ages shown in bold are considered representative, as explained in the text.

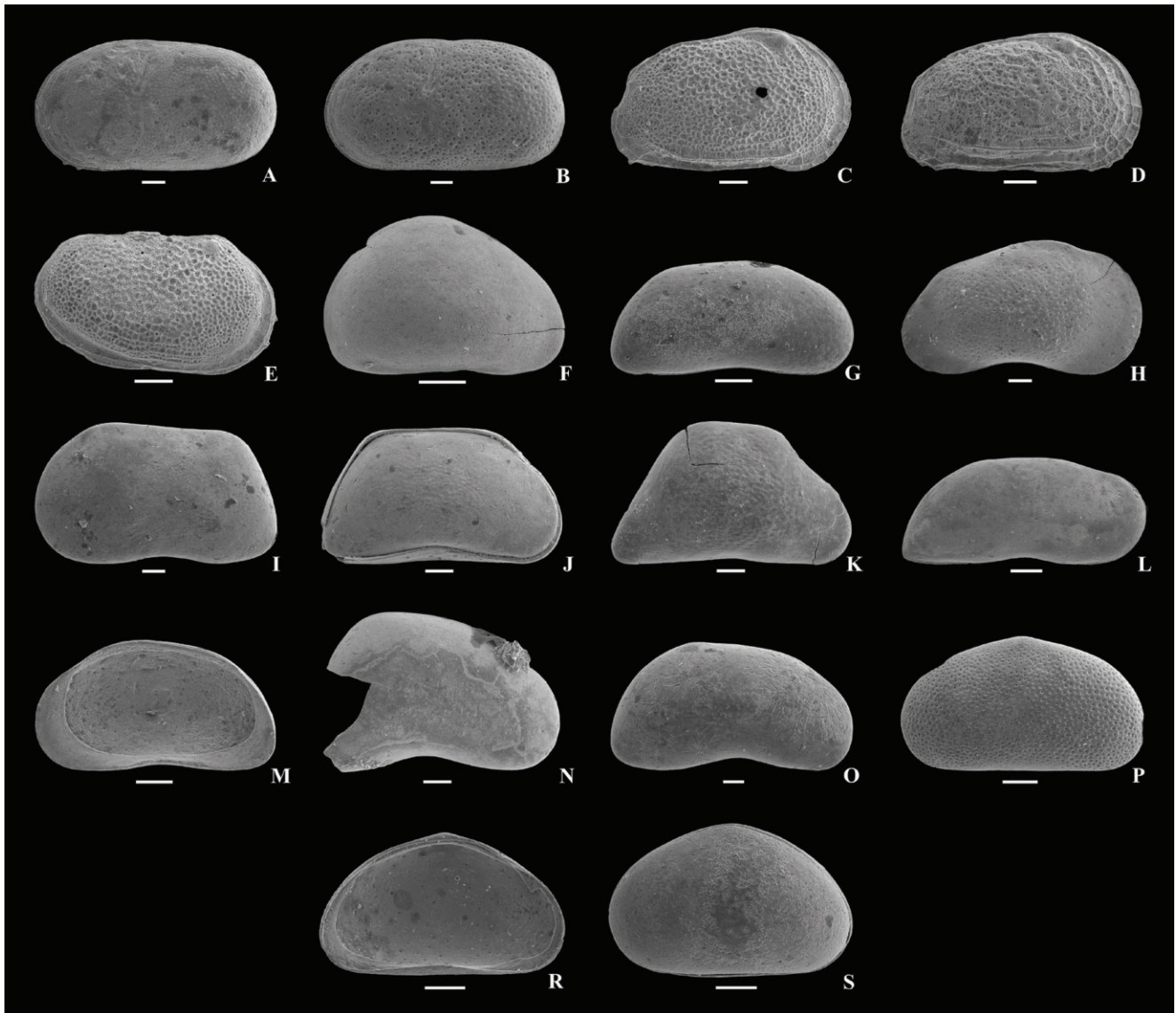


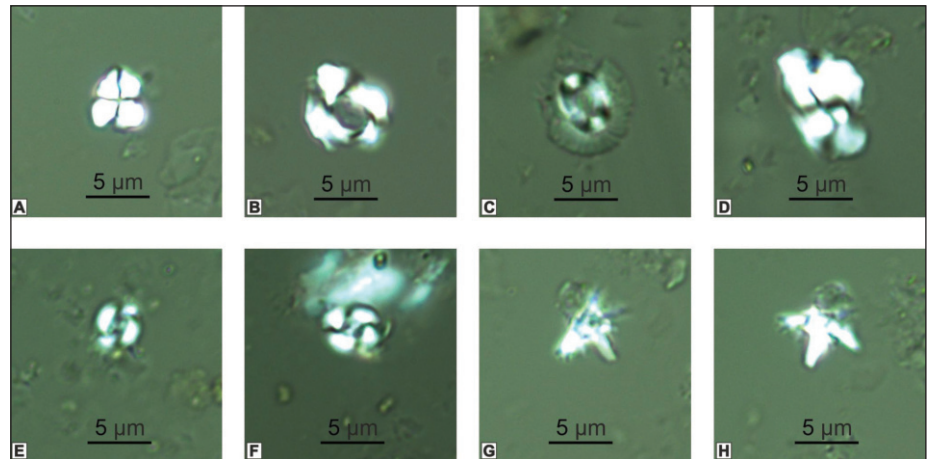
Fig. 8 - Brackish Paratethyan (A-L) and freshwater (M-S) ostracods from Outcrop A. A) *Cyprideis* aff. *obesa* (Reuss 1850), LV♀, external lateral view; B) *Cyprideis* sp., LV♀, external lateral view; C) *Hemicytheria folliculosa* (Reuss 1850), RV♀, external lateral view; D) *Hemicytheria* sp., RV♀, external lateral view; E) *Loxococoncha granifera* (Reuss 1850), C♀, external lateral view on RV; F) *Xestoleberis* sp., RV, external lateral view; G) *Amplocypris abscessa* (Reuss 1850), RV, external lateral view; H) *Herpetocyprilla auriculata* (Reuss 1850), RV juv., external lateral view; I) *Lineocypris granulosa* (Zalányi 1959), LV, external lateral view; J) *Lineocypris trapezoides* (Zalányi 1929), C♀, external lateral view on RV; K) *Lineocypris* sp., RV, external lateral view; L) *Pontoniella* sp., RV♀, external lateral view; M) *Candona* sp. 1, RV♀, internal lateral view; N) *Candona* sp. 2, RV♂, external lateral view; O) *Candona* ex gr. *neglecta* Sars, 1887, RV♀, external lateral view; P) *Pseudocandona* sp., LV, external lateral view; R) *Pseudocandona* ex gr. *eremita* (Vejdovský 1882), LV, internal lateral view; S) *Cycloocypris* sp., C, external lateral view on LV; Abbreviations: C – carapace; RV – right valve; LV – left valve; ♂ – male; ♀ – female; juv. – juvenile. Scale bar: A-F, H-S – 0.1 mm; G – 0.2 mm

sition within the profile, with an increasing input of clastic material. All three FIIT samples exhibit very similar $^{10}\text{Be}/^{9}\text{Be}$ ratios, despite the lithological changes along the profile, implying that the fine-grained material was derived from the same source and depositional process.

The depositional age calculation was performed using lacustrine ($R_{0-L} = (6.97 \pm 0.14) \times 10^{-9}$) as well as the alluvial initial authigenic ratios ($R_{0-F} = (4.14 \pm 0.17) \times 10^{-9}$), established by Šujan et al.

(2016a). This, in turn, is justified by the results of the study by Magyar et al. (2019), which showed that the calculation using alluvial initial ratio for Lake Pannon deltaic sequence systematically yielded ages in better agreement with magnetostratigraphic and biostratigraphic proxies than is the case with lacustrine initial ratio-based ages. The latter proved to be effective in the deep-water deposits of Lake Pannon, in which there was significant siliciclastic input (Botka et al. 2019).

Fig. 9 - Nannoplankton specimens collected from Outcrop B. Nannoplankton association comprises reworked Paleogene and Middle Miocene (A-D), and taxa attributed to the late Miocene (E-G). A) *Sphenolithus abies* (FIIT1); B) *Reticulofenestra pseudumbilicus* (FIIT1); C) *Coccolithus pelagicus* (FIIT1); D) *Cyclicargolithus floridanus* (FIIT1); E,F) *Reticulofenestra tegulata* (FIIT2); G) *Isolithus semenenko* (FIIT2); H) *?I. pavelici* (FIIT2).



Tab. 2 - Documented nannoplankton taxa.

Sample	Zone/Subzone	Composition
FIIT1	Redeposited material of NN6 (Sarmatian/U. Badenian), of Paleogene and Cretaceous	<i>Coccolithus pelagicus</i> , <i>Cyclicargolithus floridanus</i> , <i>Reticulofenestra minuta</i> , <i>R. pseudumbilicus</i> , <i>R. haqii</i> , <i>Sphenolithus abies</i> , <i>Pontosphaera multipora</i> , <i>?Discoaster adamanteus Triquetrorhabdulus sp.</i> , <i>Coccolithus formosus</i> , <i>Cyclicargolithus abisectus</i> , <i>Reticulofenestra bisecta</i> , <i>Broinsonia parca parca</i> , <i>Micula staurophora</i> , <i>Prediscosphaera cretacea</i> , <i>Retecapsa crenulata</i> , <i>Watznaueria barnesae</i>
FIIT2	?NN9 equivalent/ Pannonian; redeposited material of NN6 (Sarmatian/Badenian) and Cretaceous	<i>Isolithus semenenko</i> , <i>?I. pavelici</i> , <i>Reticulofenestra tegulata</i> , <i>C. floridanus</i> , <i>R. haqii</i> , <i>R. minuta</i> , <i>W. barnesae</i>
FIIT3	Indeterminate	barren, clay minerals

The depositional ages of the FIIT samples calculated in the described way range between 12.07 ± 0.75 Ma and 12.42 ± 1.02 Ma (R_{0-1}), and 11.03 ± 0.82 Ma and 11.37 ± 1.04 Ma (R_{0-1V}). The single population appearance of the FIIT samples allowed for the calculation of the weighted mean ages using the approach of Spencer et al. (2017), yielding values of 12.22 ± 0.55 Ma (R_{0-1}) and 11.19 ± 0.58 Ma (R_{0-F}). The depositional ages of samples MA-1-153 and VO-5-51.8 resulted in somewhat lower ages of 11.57 ± 1.06 Ma and 11.09 ± 1.00 Ma (R_{0-1}), and 10.52 ± 1.06 Ma and 10.04 ± 1.00 Ma (R_{0-F}), respectively. Since both samples were taken from the same stratigraphic level, their weighted mean ages could be calculated: 11.32 ± 0.73 Ma (R_{0-1}) and 10.27 ± 0.73 Ma (R_{0-F}), respectively.

The weighted mean age of FIIT samples calculated using the lacustrine initial $^{10}\text{Be}/^9\text{Be}$ ratio is older than 11.6 Ma (Middle/Late Miocene boundary). Nevertheless, all biostratigraphic proxies pointed to a Late Miocene age for the section. Hence, the ages calculated using the alluvial initial ratio may be considered representative, in agreement with evi-

dence for a significant terrestrial input of sediment into the paleoenvironment. This approach is analogous to the application of authigenic $^{10}\text{Be}/^9\text{Be}$ dating to deltaic deposits by Magyar et al. (2019).

The high degree of uncertainty associated with the ages is linked to the high analytical uncertainty values (6–11%), but can be explained by the low $^{10}\text{Be}/^9\text{Be}$ ratios resulting from ages, reaching from ~ 7.2 to 8.5 times the half-life of ^{10}Be (1.387 ± 0.012 Ma; Chmeleff et al. 2010; Korschinek et al. 2010), which is close to the lower boundary of the method's applicability (~ 14 Ma; Bourlès et al. 1989).

Shallow seismic survey

Description. The shallow refraction seismic survey resulted in the seismic velocity models, which served for the calculation of the velocity tomographic profiles depicted in Fig. 10. Three distinct sub-horizontally arranged horizons with different velocity properties were documented in seismic section 1 (Fig. 10A). The upper horizon (1) represents an environment with low velocity, that is, with values of $<500 \text{ m}\cdot\text{s}^{-1}$. This horizon is 4.5–9.0 m thick

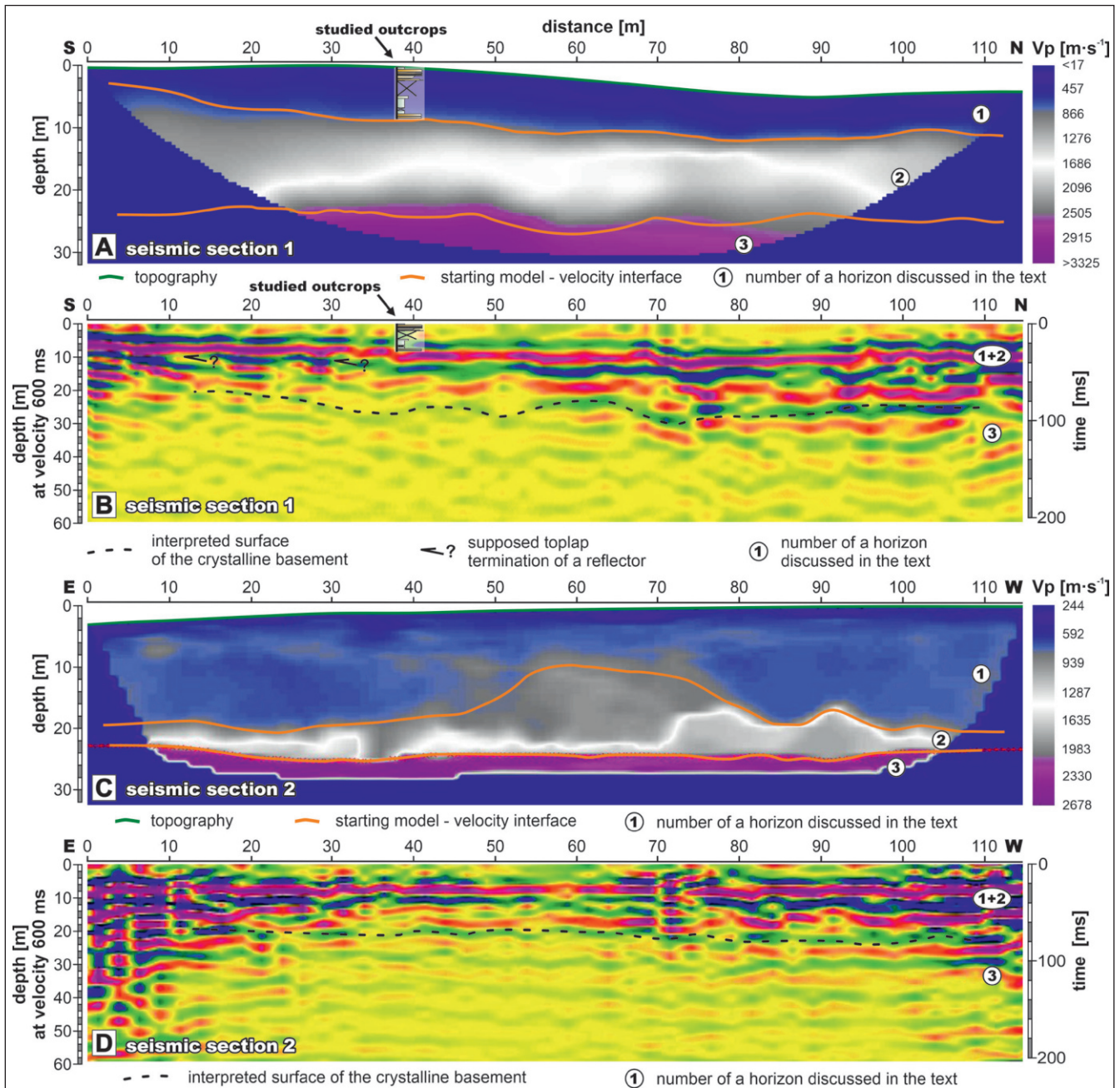


Fig. 10 - Shallow seismic survey. A, C) Seismic refraction tomography – velocity profiles; B, D) seismic reflection profiles. It should be noted that the vertical scale is different for refraction tomography and reflection seismic profiles. “?” indicates potential clinoforms. For the location of the sections see Fig. 3. For details of the studied outcrops, see Fig. 4.

with a slightly inclined and gently truncated base. A 12–16 m thick horizon (2), with seismic velocities in the range of 1100–1300 $\text{m}\cdot\text{s}^{-1}$, is situated below. The transition to the third horizon appears to be significantly truncated. The lowermost horizon (3) occurs at depths 20–25 m and exhibits an average seismic velocity of 3600 $\text{m}\cdot\text{s}^{-1}$. Seismic section 2 shows the presence of three horizons with seismic velocity properties comparable to that of section 1, although with a different geometry of the boundaries (Fig.

10C). The upper horizon (1) is 10–20 m thick with seismic velocity values of <600 $\text{m}\cdot\text{s}^{-1}$, and is divided from the underlying horizon (2), which has a seismic velocity range of 1,000–1,500 $\text{m}\cdot\text{s}^{-1}$, by a complicated boundary with convex-upwards feature between 45 and 85 m of the section length. The boundary appears at various depths, reaching 9–20 m. The boundary towards the lowermost horizon (3), which has a seismic velocity of >2,600 $\text{m}\cdot\text{s}^{-1}$, is planar without major truncations.

The reflection seismic images allow for the observation of geometries on the scale of >3.5 m, which is the average thickness of a single reflector (Fig. 10B, D). Section 1 displays continuous sub-horizontal high-amplitude reflectors within horizons (1) and (2), which could not be differentiated (Fig. 10B). Supposed toplaps between the sub-horizontal and underlying gently inclined reflectors were observed at a depth of 10 m and section length of 10–35 m. A transition to an environment with chaotic to low-amplitude reflectors (horizon 3) could be seen at a depth of 20–25 m, and this exhibited a truncated morphology. The lowermost reflectors of the horizon (1+2) appear to follow the morphology of the boundary towards horizon (3). The same boundary between the high-amplitude sub-horizontal reflectors (horizons 1+2) and underlying chaotic to low-amplitude reflectors (horizon 3) can be seen in section 2 (Fig. 10D), with, however, a gentle morphology without truncations.

Interpretation. The seismic velocity of horizon (1) falls within the range of values characteristic of a loose sandy, or sandy-gravelly environment; in horizon (2) seismic velocity is associated with an environment predominantly composed of poorly compacted clays and silts; horizon (3) exhibits seismic velocities which may be interpreted as representing strongly weathered granitoids (e.g., Bourbié et al. 1987). Those horizons with comparable lithology were located in boreholes drilled in close proximity to the seismic survey (Fig. 3). Despite the seismic velocity values, the direct outcrop observations specify that horizon (1) contains a significant proportion of muddy facies, in addition to sand and gravel. The supposed muddy horizon (2) was not reached by the excavations, but reflection seismics shows their sub-horizontal geometry conformably covering the locally truncated weathered granites, with a possible presence of clinofolds in Fig. 10B. The convex-upwards feature of horizon (2) observed in Fig. 10C does not appear to be limited by reflectors in Fig. 10D, but the reflectors are continuous across this feature. This implies that the anomaly is represented by lateral lithological transitions between mud-prone Miocene strata in the middle of the anomaly and correlative sandy-gravelly deposits on both sides.

Correlation with borehole logs

In relation to the outcrops under consideration, the upper Miocene succession is distributed

in the broader vicinity of the excavations, reaching a thickness of at least 40 m (range 157.5–197.5 m a.s.l., Fig. 3C). The succession is mostly composed of subaquatic muds without signs of subaerial exposure, except for in well T-10. Sandy and gravelly strata are present at the base of the succession (well S-9) and close to buried slopes of pre-Cenozoic granitoids (wells CH1-3, T-11, T-32), and represent less than 20% of the overall thickness. The distribution and genetic character of the overlying colluvial/eolian and river terrace Quaternary deposits implies that the upper Miocene succession in question represents an erosive remnant located on a moderately sloping hill which survived incision by streams in surrounding valleys during the Pleistocene.

DISCUSSION

Paleoenvironment

The mollusk and ostracod specimens were found *in situ* within strata of massive silt and bioturbated sand. The shallow infaunal, lacustrine lymnocypridines are associated with a brackish water environment (Albrecht et al. 2014). Paratethyan ostracods lived in a brackish environment ranging from 2‰ to 16‰ (Cziczter et al. 2009). They achieved the highest degree of species abundance in the open sublittoral limnic environment, in which trapezoidal and elongated Candonidae and Leptocytheridae dominated (Cziczter et al. 2009; Barna et al. 2010). The ostracod species associations changed towards the lake shore and consisted of Paratethyan taxa and freshwater species coming from marshes, oxbows, estuaries, and ephemeral lakes (Pipík et al. 2013). Outcrop A contains the robust, large, heavy calcified valves and carapaces of two *Cyprideis* species, which prevail over the large, flat valves of Cyprididae and Candonidae. Their dominance probably results from higher resistance to transport and lithostatic pressure compared with that of Cyprididae and Candonidae; it was not therefore possible to calculate species dominance. The robust *Cyprideis* taxa occurred mostly in the sublittoral environment of Lake Pannon (Pipík et al. 2007). This bathymetrical assumption for Outcrop A is supported by the presence of elongated, pointed in posterior valves of *Pontocyprilla* and trapezoidal valves of *Lineocypris* which are frequently observed in sublittoral and profundal biotopes of Lake Pannon (Cziczter

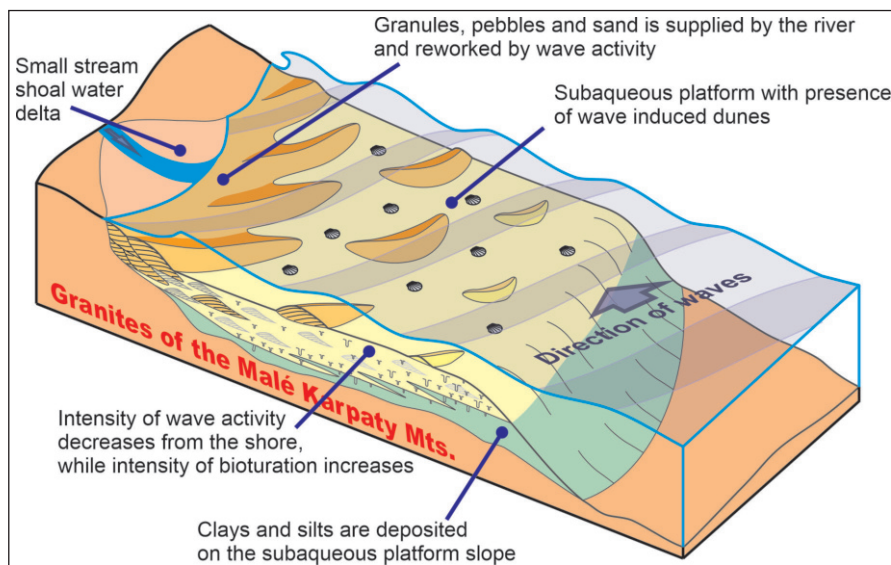


Fig. 11 - Block diagram showing the depositional processes and paleoenvironment of the outcrops – a shoal water delta formed during transgression of Lake Pannon.

et al. 2009; Pipík et al. 2012). On the other hand, the number of carapaces indicates a higher rate of sedimentation, although it relates to the taxa with an adont hinge (Candoninae, Cyprididae), which makes examples of these taxa prone to the separation of the valves after the death of an individual (Oertli 1971). This fact, together with the presence of freshwater taxa, suggests the proximity of the coast. Chalky and frequently damaged valves with abraded margins and surfaces probably represent the results of mechanical transport or prolonged exposure before final burial (Kontrovitz 1967; Kaesler et al. 1993). Thus, the ostracods confirm the supposition of fine clastic deposition between the open sublittoral to marginal littoral environments influenced by freshwater fluvial transport.

Skolithos ichnofacies is a typical trace fossil of shallow marine environments with relatively high water current energy (Knaust 2017). *Arenicolites* can indicate a shallow marine environment influenced by stress factors, similarly to the *Skolithos* ichnofacies opportunistic trace fossil association (Bromley and Asgaard 1991). *Ophiomorpha* appears in a wide range of environments and could be accompanied by *Skolithos* ichnofacies association in brackish water environments (Leaman et al. 2015; Gingras et al. 2012). The simple morphology of the *Planolites* ichnofacies ensures its predisposition to a wide range of environmental and stratigraphic situations (Knaust 2017). Large, branched and chambered burrows of shrimps related to the *Thalassinoides* ichnofacies observed in this research were described from the Late Miocene lacustrine-deltaic sequence

of the Bzenec Formation of Lake Pannon (Hyžný et al. 2015).

Hence, the association of trace fossils found in massive sand, in faintly laminated sand and in dunes implies a dynamic environment. The currents responsible for the formation of dunes were most probably induced by wave action, as indicated by the ichnofauna and sorting of the sediment (Dumas and Arnott 2006; Pemberton et al. 2012; Vakarelov and Ainsworth 2013; Rossi et al. 2017). In opposition to dune sediment, the faintly cross-bedded and massive sandy gravel and gravelly sand was deposited by short, local streams sourced by eroded granites onto a lake shore as a shoal water delta front (Fig. 11) (García-García et al. 2006; Ghinassi 2007). The surge-type flows achieved a more distal nature via the deposition of planar sandy beds with muddy lenses, transporting fine clastic particles and light ostracod valves in suspension up to the prodelta settings. The presence of a shoal water delta environment is also implied by the simple horizontal reflector geometry of the sandy-gravelly strata in the order of ~3 m thickness seen in reflection seismic profiles and in the absence of clinoform geometry.

The deposition of clays and silts took place in an environment of slow currents and/or suspension below the wave base, but relatively close to the terrestrial source of abundant plant detritus, most probably on the slope of a subaqueous platform associated with the shoal water delta (Fig. 11). It is this which might be indicated by supposed on-laps of clinoform geometry in Fig. 10A (Patruno & Helland-Hansen 2018). The granitic massif would

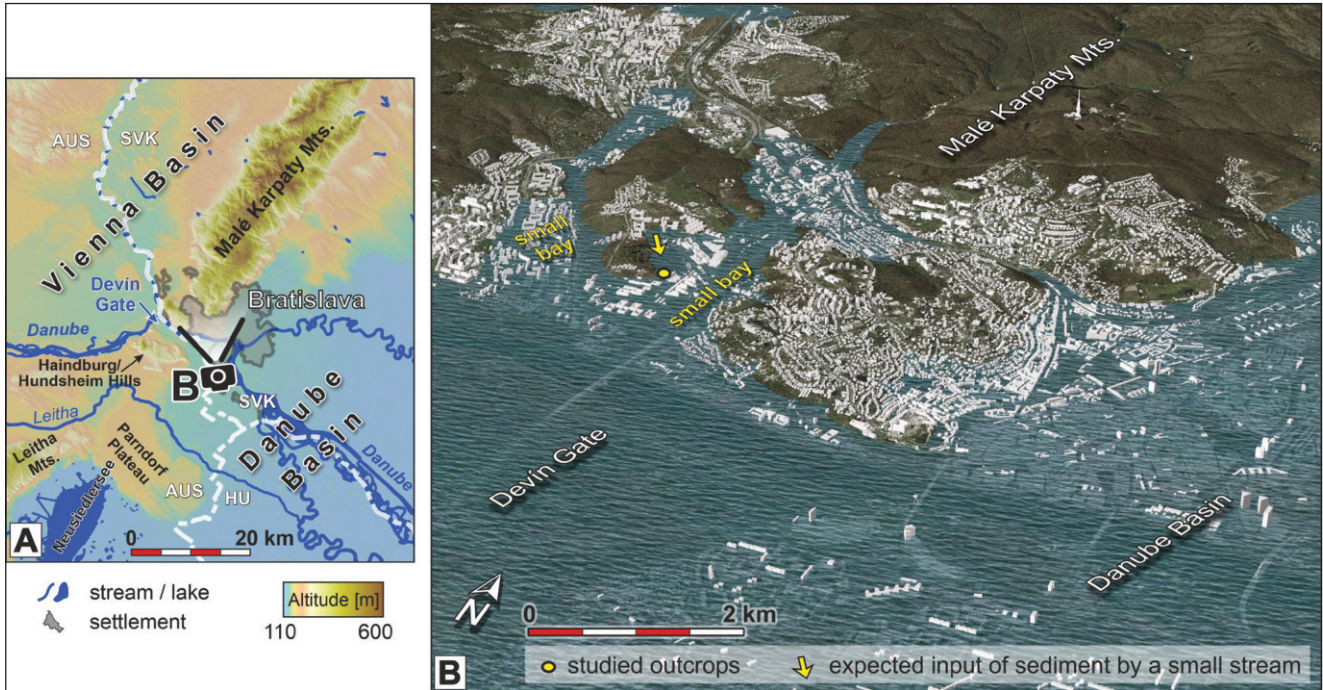


Fig. 12- A) Location of the panoramic view on the present-day topography. B) Panoramic artistic view on the paleogeography of the studied locality at ca. 10.5 Ma using present topography of the area (Sujan 2019, modified).

not supply the short stream with a high amount of muddy sediment, which forms >50% of the succession in the outcrops and even >80% in the nearby archival well-cores (Fig. 3). The nannoplankton association in samples FIIT1 and FIIT2 and ostracods from Outcrop A clearly indicate that the fine-grained material was derived from the erosion and redeposition of contemporaneous and Middle Miocene deposits (NN6; Martini 1971), which are still preserved in the vicinity of the studied area (Fig. 2). The rich presence of nannoplankton taxa characteristic of the Paleogene and Cretaceous periods implies that either their accumulations were much more extensive during the Late Miocene compared to present, or that these specimens experienced multiple recycling phases.

The rapid alteration between those facies accumulated below the wave base, riverine stream facies and wave-reworking facies indicates that the depth of the wave base, and hence wavelength, was limited. This is in good agreement with the position of the locality under consideration, which most probably took shape on the shore of a small bay, as shown in Fig. 12. The narrow morphology of the bay, surrounded by the hills of the pre-Cenozoic massif, confined the wave activity, which would have been much greater on an open coast of Lake Pannon (e.g., Sztanó et al. 2013). The intercalation

of shoal water delta facies and open lacustrine muds observed in the outcrops is characteristic of transgressive deposits (Ghinassi 2007; Helland-Hansen & Hampson 2009), in this representing the transgression of Lake Pannon above the Malé Karpaty Mts.

Age of deposition

The taxon *Lymnocardium* is endemic to Lake Pannon and indicative of a Late Miocene age. The presence of *Lymnocardium* cf. *conjungens*, and *Lymnocardium* cf. *schedelianum* reveals a probable time window for the deposition of these sediments within the Pannonian letter stages D and/or E (Papp et al. 1985), with a rough age constraint of ~10.6–10.1 Ma (Fig. 13) (Harzhauser et al. 2004). However, the same *Lymnocardium* taxa represent biozones with time slightly broader constraints, defined for the Danube Basin as ~10.9–10.3 Ma and 10.9–9.6 Ma, respectively (Fig. 13) (Magyar et al. 2007; Sztanó et al. 2016). In particular, *L. schedelianum* was present in littoral environments of Lake Pannon until even ~9.6 Ma, while in the sublittoral zone it evolved into *L. soproniense* Vitális 1934 at ~10.3–10.2 Ma (Magyar et al. 2016). Therefore, its concurrent presence with *L. conjungens* which then extends the possible time constraints in the studied succession to ~10.9–9.6 Ma.

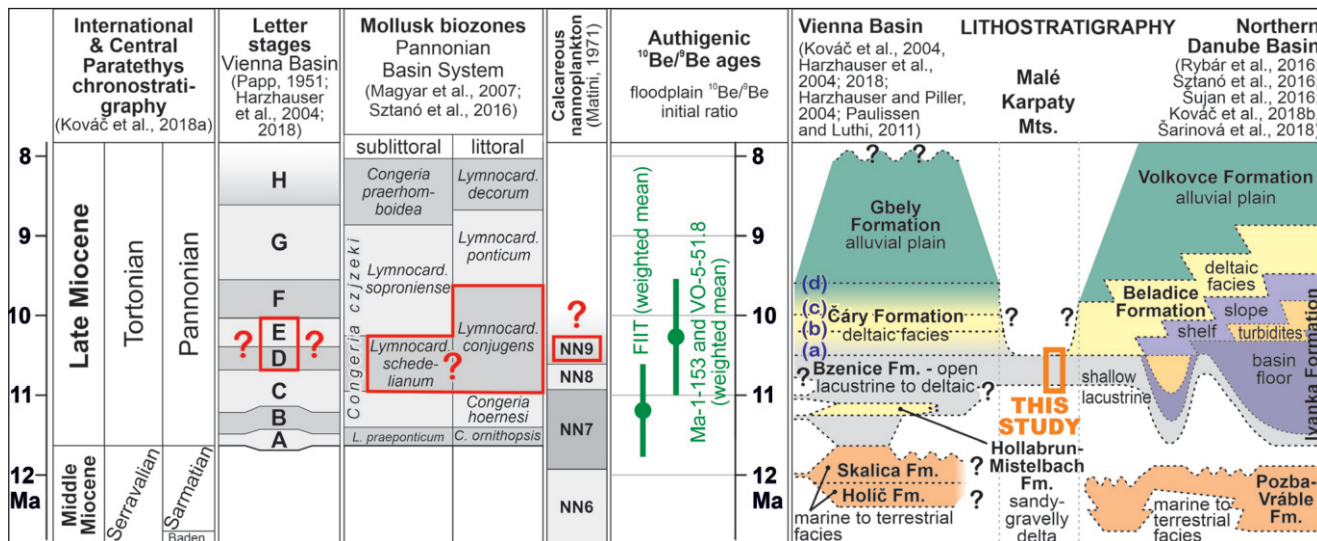


Fig. 13 - Stratigraphic scheme summarizing the data collected and showing the expected position of the succession featured in this study. Boundaries of the upper Miocene succession in the Vienna Basin: (a) – base of the deltaic Čáry Fm. (Paulissen & Luthi 2011); (b) – base of the deltaic Čáry Fm. (Harzhauser et al. 2004); (c) – base of the alluvial Gbely Fm. (Paulissen & Luthi 2011); (d) – base of the alluvial Gbely Fm. (Harzhauser et al. 2004). Lithostratigraphy of the Danube Basin according to Sztanó et al. (2016). A question mark in biostratigraphy means that the determination allows only for a tentative correlation with a biozone. A question mark in lithostratigraphy indicates the absence of data regarding the presence of the correlative deposits, or the absence of a depositional age.

Of the ostracods, *Herpetocyprilla auriculata* was identified in the lower Pannonian of the Vienna Basin, but the genus also occurs in the younger Lake Pannon strata. *Amplocypris absissa*, *Hemicytheria folliculosa* and *Loxococoncha granifera* allow the succession to be attributed to the regional Pannonian letter stages D and E, *sensu* Papp (1951). *Cyprideis* aff. *obesa* is similar to the large sublittoral *C. obesa* and *C. sublittoralis* of the Pannonian lithostratigraphic stage E, but it differs from *C. obesa* in outline and from *C. sublittoralis* in the details of the hinge composition. The individuals from Outcrop A have, therefore, been left in an open nomenclature (Jiríček 1985).

The nannoplankton assemblage of sample FIIT1 included no index fossil, but species common in Middle Miocene (upper Badenian, Sarmatian) *Coccolithus pelagicus*, *Cyclicargolithus floridanus*, *Reticulofenestra minuta*, *R. pseudounbilicus*, *R. haqii*, *Sphenolithus abies*, *Pontosphaera multipora*, *?Discoaster adamantus* and *Triquetrorhabdulus* sp. together with species characteristic of the Paleogene *Coccolithus formosus*, *Cyclicargolithus abisectus*, *Reticulofenestra bisecta*, and Cretaceous, *Broinsonia parca parca*, *Micula staurophora*, *Prediscosphaera cretacea*, *Retecapsa crenulata*, *Watznaueria barnesae*. Despite the fact that sample FIIT1 might be tentatively assigned to NN6 Zone on the basis of its overall assemblage (Martini 1971), its affinity to the upper Miocene strata clearly points to the redeposited character of the specimens derived from

various sources. The presence of *Isolithus semenenko* (Lyuřeva 1989) (sample FIIT2) is representative for the Late Miocene age (Fig. 13), and according to the approach of Lyuřeva (1989) and Kováč et al. (2006), might be considered an indication of the NN9 biozone. However, it has also been documented in a wider age window across Lake Pannon (11.6–8.9 Ma) and potentially also in the Middle Miocene deposits of the Central Paratethys (Ćorić 2006; Reischenbacher et al. 2007; Cziczter et al. 2009; Galović 2017) and in the deposits of the Pontian age located in the Taman peninsula (Radionova et al. 2012), all of which makes only the correlation to the Late Miocene age robust. The other species present in sample FIIT2 are redeposits of the Middle Miocene, namely *C. floridanus*, *R. haqii*, and *R. minuta* and Cretaceous reworking represented by *W. barnesae*.

The authigenic $^{10}\text{Be}/^9\text{Be}$ age determinations were performed using both lacustrine and alluvial initial ratios, since both proved useful in the analysis of the Lake Pannon deposits (Šujan et al. 2016a; Botka et al. 2019; Magyar et al. 2019). Nevertheless, the alluvial initial ratio-based weighted mean age of 11.19 ± 0.58 Ma overlaps the time span constrained by the biostratigraphic proxies, and hence, is assumed to be the relevant one. The facies inventory implies a nearby terrestrial source of sediment. The time frame under consideration was characterized by the presence of the extensive paleo-Danube del-

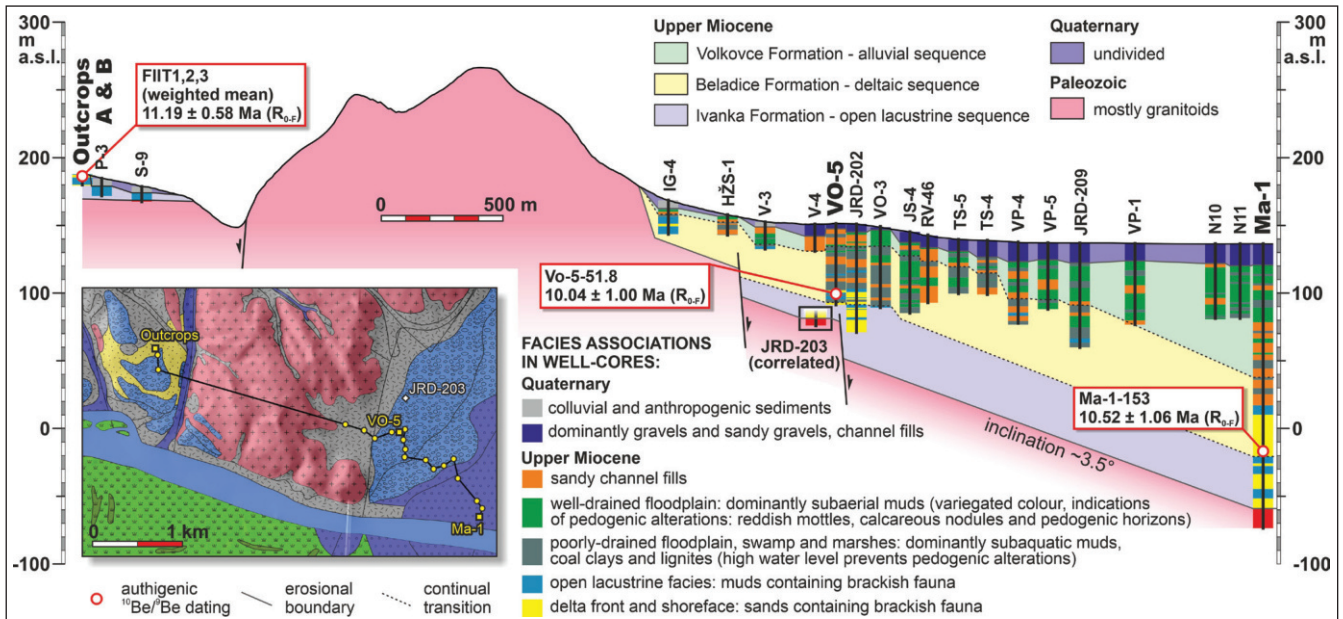


Fig. 14 - Correlation of the studied outcrops with boreholes situated on the Danube Basin margin. Note the $\times 5.5$ vertical exaggeration of the geological section. Borehole JRD-203 is situated 320 m to the north of the section. For explanations of geology on the location map see Fig. 2.

ta in the Vienna Basin (Fig. 13), and this prograded close to the Malé Karpaty Mts. (Fig. 1) (Harzhauser et al. 2004). This deltaic body might have affected the initial isotopic ratio found in the Lake Pannon water column as the source of an increased input of terrestrial ^9Be . Thus, taking the biostratigraphic and authigenic $^{10}\text{Be}/^9\text{Be}$ results as a guide, the age of deposition of the succession falls within the period $\sim 10.9\text{--}10.6$ Ma.

Lithostratigraphic position and implications for paleogeography

The origin of the succession as transgressive facies is in accord with the gradual flooding of Lake Pannon margins (Magyar et al. 2013; Sztanó et al. 2016), a process which reached its greatest extent in the Vienna Basin at ~ 10.5 Ma (Harzhauser et al. 2003; Harzhauser & Mandić 2004). Subaerially exposed and gradually flooded basin margins formed by a pre-Cenozoic massif were truncated by erosion and formed the bays of Lake Pannon in the area of the Malé Karpaty Mts. in the study area (Fig. 10). Comparable strata have been described as Kisbér Mb. within the sublittoral lacustrine muddy Szák Fm. in the foothills of the Transdanubian Range (Budai & Fodor 2008; Sztanó et al. 2016). Deposits which correlate to the Szák Fm. have been assigned to the Ivanka Fm. in the Slovakian part of the Danube Basin, and equivalent to the Bzenice Fm. of the

Vienna Basin (Fig. 13). Hence, the succession under examination here should be included in the Ivanka Fm. (Sztanó et al. 2016).

The depositional record was correlated with succession on the northwestern margin of the Danube Basin on the basis of information from boreholes acquired from archival reports and published data (Fig. 14). The whole upper Miocene succession appears to be tilted towards the basin center with inclination of $\sim 3.5^\circ$, a finding similar to those was observed in other studies of the region (Šujan et al. 2016b; Šujan et al. 2018b; Joniak et al. 2020). Post-depositional tilt due to Pliocene basin inversion is a common feature of the margins of Pannonian Basin System depocenters (e.g., Horváth et al. 2006).

The depositional record made it possible to distinguish three upper Miocene formations overlaid discordantly by the Quaternary gravels of mostly fluvial origin. Since only a few boreholes in the area penetrated the pre-late Miocene basement (Ma-1 and JRD-203 situated nearby the section), the figure $\sim 20\text{--}50$ m for the thickness of lowermost open lacustrine Ivanka Fm. is only a tentative estimate (Fig. 14); it consists solely of muddy open lacustrine facies and of sandy delta front and shoreface deposits, containing dominantly brackish fauna (Fordinál and Tuba 1992; Fordinál 1995; Nagy et al. 1995; Fordinál and Harčová 1997). The open lacustrine deposits of the Ivanka Fm., which are generally coeval with

the outcrops studied here, contain shells of *Congeria* (*Trigonipraxis*) *martonfii* Lörenthey 1893, *Lymnocardium spinosum* Lörenthey 1902, *L.?* *promultistriatum* Jekelius 1944, *Parvidacna tinnyeana* (Lörenthey 1906) and *P.?* *turislavica* (Jekelius 1944) in the well-core of Ma-1 (Nagy et al. 1995). This stratigraphic interval was assigned by Nagy et al. (1995) to the lithostratigraphic stage C of the Vienna Basin according to Papp (1951) and Rögl et al. (1993), with an age range of ~11.2–10.7 Ma (Harzhauser et al. 2004). Fordinál & Tuba (1992) documented mollusk fauna characteristic of lithostratigraphic stage D (~10.7–10.4 Ma, Harzhauser et al. 2004) at the base of upper Miocene deposits in well-core JRD-203. This is located closer to the basin margin (Fig. 14), a fact which agrees with the expected age of the transgressive sequence studied here. The open lacustrine Ivanka Fm. shown to be present in Fig. 14 could be considered as correlative to the lower part of the succession which is seen to outcrop in the Pezinok claypit located ca. 20 km to the northeast (Fig. 2C), where occurrence of *Congeria* (*Coelogonia*) *gitneri* Brusina 1892 recorded by Fordinál (1993) points to an estimated age of ~11.2–10.1 Ma (lithostratigraphic stages C–E, Papp 1951, Harzhauser & Mandić 2010). It is worth mentioning that the Lake Pannon transgression of deep basin depocenters appeared much earlier, at the beginning of the Late Miocene at ~11.6–11.4 Ma, as indicated by mollusk fauna and dinoflagellates from the Danube Basin well-cores (Magyar et al. 2007).

The gradual regression of Lake Pannon is recorded by deposition of the deltaic Beladice Fm., reaching a thickness of ~60 m in the section considered here (Fig. 14). It consists of terrestrial, poorly drained floodplain facies, originating in a landscape with marshes and swamps, as well as deltaic channels, and also the open lacustrine facies included in the Ivanka Fm. The Beladice Fm. contains mollusk fauna characteristic of brackish to freshwater environments (Fordinál 1995; Nagy et al. 1995; Pipík 1998). Species related to the transition from an open lacustrine to a deltaic environment in the core Ma-1 include *Lymnocardium conjungens* (Hörnes 1862), *Dreissena* (*Modiolodreissena*) *auricularis* (Fuchs 1870), *Congeria* (*Andrusoviconcha*) *neumayri* Andrusov 1897, *Melanopsis bouei* Férussac 1823, and *Melanopsis austriaca* Handmann 1882. The occurrence of these species is typical of the regressive deltaic succession of Lake Pannon documented in the Pezinok claypit (Fordinál 1997) (Fig. 2C), and was observed in the

correlative Čáry Fm. in the Vienna Basin (Harzhauser et al. 2004). The anagenetic evolution of *Dreissena* (*Modiolodreissena*) *auricularis* from *Congeria* (*Coelogonia*) *gitneri* was suggested by Papp (1950) and implies that the regression marked by deposition of the deltaic Beladice Fm. appeared in the area of well Ma-1 and in the upper part of the Pezinok outcrop (Horusitzky 1907) within a time frame of ~10.1–9.65 Ma (lithostratigraphic letter stage F, Harzhauser et al. 2004). The two dating results of samples Ma-1-153 and VO-5-51.8 from boreholes Ma-1 and VO-5 displayed floodplain initial ratio-based authigenic $^{10}\text{Be}/^9\text{Be}$ ages of 10.52 ± 1.06 Ma and 10.04 ± 1.00 Ma, respectively (Table 3; Fig. 14). The samples are placed just above the base of the deltaic Beladice Fm. and their mean weighted age of 10.27 ± 0.73 Ma agrees with start of the Lake Pannon regression after it had reached its greatest extent; this is also indicated by the other proxies mentioned above. Hence, the regression phase of Lake Pannon in the area of Bratislava could be constrained to ~10.2–10.0 Ma.

The regression in the study area appeared simultaneously with alluvial deposition in the localities of Haslau and Götzendorf in the western part of the Vienna Basin (Fig. 2C) (Harzhauser et al. 2004; Harzhauser & Tempfer 2004). The regressive deltaic system was still far from the Sopron-Eisenstadt Basin located ca. 70 km to the southwest, since offshore conditions with deposition of Szák Fm. muds appeared in the area of the at ~10.0 Ma, as indicated by magnetostratigraphy and presence of *Lymnocardium soproniense* specimens in the Sopron claypit (Fig. 2C) (Magyar et al. 2007). The regressive deltaic system appeared there later, at ~9.7–9.5 Ma according to the magnetostratigraphic and mollusk biostratigraphic data (Magyar et al. 1999).

The fault displacement is modest, reaching offsets of 20–30 m, tentatively documented on the basis of borehole correlation and the altitude of the Ivanka Fm. on the Danube Basin margin, and in the outcrops seen in Fig. 14. Thus, the syn- and post-Late Miocene activity of these normal faults was of low intensity. The structures should be related to the SW-NE trending Malé Karpaty fault (Marko and Jureňa 1999; Lenhardt et al. 2007), which exhibits a much higher degree of offset – in the order of hundreds of meters – further to the northeast (Joniak et al. 2020). It is reasonable to assume that this fault branches out into a fault system of structures with smaller slip in the area of Bratislava.

The information gained in this study implies, that the pre-Cenozoic massif in the area of Bratislava was passively flooded by Lake Pannon transgression, becoming an archipelago. Considering the thickness of correlated formations, the granitic hills must also have been partly exposed during the Lake Pannon regression. The paleo-Danube river channels branched around the exposed hills and the Malé Karpaty Mts. might have been fully covered only later by the alluvial Volkovce Fm., which accumulated up to ~6.0 Ma (Sztanó et al. 2016; Šujan et al. 2016a). As may be seen in Fig. 13, the timing of changes between sedimentary formations during the Late Miocene, recorded as gradual shifts of depositional systems, is relatively well defined for the Danube Basin (Sztanó et al. 2016; Šujan et al. 2016a; Šarinová et al. 2018). However, there are inconsistencies and uncertainties in the lithostratigraphy of the upper Miocene sequence of the Vienna Basin related to the transition from open lacustrine to deltaic and alluvial settings. Harzhauser et al. (2004) constrained the timing of the change from open lacustrine to deltaic environment to ~10.2 Ma, and subsequently to an alluvial environment at ~9.6 Ma. Nonetheless, constraints based on magnetostratigraphy by Paulissen and Luthi (2011) imply ~10.5 Ma and ~10.0 Ma, respectively, for the same paleoenvironmental shifts. Kováč et al. (1998) even suggested erosional contact between the alluvial Gbely Fm. and deltaic Čáry Fm., which is well documented in marginal settings (e.g., Jelínek et al. 2011), but not expected in the central part of the basin. The existing lithostratigraphic models do not include time-transgressive boundaries of the formations. If the paleo-Danube delta represented one migrating depositional system, the final regression in the Vienna Basin had to appear before or at the same time as it took place on the NW margin of the Danube Basin (~10.0 Ma). Hence, it is a matter for future research to specify the timing of these transitions and their temporal and spatial differences.

Broader context within the Pannonian Basin System

The settings observed are specific compared to Lake Pannon transgressions documented in other locations. Extensive swamps, marshes and alluvial plains were present on the northwestern margin of the early Lake Pannon (Vienna and Styrian basins; Fig. 2B), with a high sediment supply from the Eastern Alps, and were gradually replaced at ~11.3–10.5

Ma by an open lake environment due to a water level rise (Harzhauser et al. 2003; Gross et al. 2011). The area of the city of Vienna experienced several short floodings separated by subaerial exposure during the same period (Harzhauser et al. 2018). The margins of the Sopron-Eisenstadt Basin experienced transgression as early as ~11.5–11.2 Ma in the locality St. Margarethen (Fig. 2C) (lithostratigraphic stage B, Harzhauser et al. 2002). The study area between the Vienna and Danube basins was flooded by transgression shortly afterwards at ~10.9–10.6 Ma, while regression occurred at ~10.2–10.0 Ma according to the present study.

Transgression appeared later, at ~9.5–9.2 Ma, in the area of the Transdanubian Range (Fig. 2B) (Cziczter et al. 2009), and transgressive depositional settings comparable to those of the present study have been documented for this time (Budai and Fodor 2008; Csillag et al. 2010). The paleo-Danube depositional system reached the area at ~8.6 Ma and regressive deltaic deposits covered the massif (Magyar et al. 2013; Bartha et al. 2014; 2015; Sztanó et al. 2016).

Investigation of the Paks well-cores in the central Great Hungarian Plain (Fig. 2B) implies that the Németskér and Tolna basement highs were flooded by transgression later than the surrounding troughs, at ~8.9–8.4 Ma according to the results of nannoplankton biostratigraphy, magnetostratigraphy and authigenic $^{10}\text{Be}/^9\text{Be}$ dating (Magyar et al. 2019). The regressive deltaic system approached the area shortly afterwards, at some point after ~8.4 Ma.

The massif of the Mecsek Mts. further to the south (Fig. 2B) was partly flooded by the earliest Lake Pannon at the Middle/Late Miocene boundary (Sebe et al. 2019). An event of subaerial exposure was followed by the transgression after ~8.0 Ma, and an open lacustrine environment had ceased to exist by the onset of the paleo-Danube depositional system at ~7.3–6.8 Ma (Kovács et al. 2018; Budai et al. 2019).

All the areas mentioned experienced the pattern of water level rise, which shortly (~1 Ma) preceded the overall regression due to the paleo-Danube shelf progradation. The pattern might be explained by sedimentary loading-induced subsidence due to the prograding shelf slope depositional system and progressive basin filling (Gvirtzman 2001; Karpytchev et al. 2018). This effect might have caused a relative base-level rise in front of the advancing depositional

system, which accumulated a sequence of turbidites, shelf slope and deltaic deposits up to 1.5 km thick in most of the Pannonian Basin System depocenters (e.g., Uhrin and Sztanó 2012; Balázs et al. 2018).

CONCLUSIONS

The present study focuses on the upper Miocene deposits, exposed above the pre-Cenozoic basement of the Malé Karpaty Mts. between the Vienna and Danube basins. According to biostratigraphic data and authigenic $^{10}\text{Be}/^9\text{Be}$ dating, the shoal water delta sandy-gravelly facies alternating with wave-induced dunes and open lacustrine muds represents a succession formed by the Lake Pannon transgression within a time frame of $\sim 10.9\text{--}10.6$ Ma. The data acquired imply that the surrounding granitic massif formed an archipelago and was sub-aerially also exposed during the following regression of the paleo-Danube deltaic system, which took place at roughly $\sim 10.2\text{--}10.0$ Ma. Fault displacement played a minor role in forming the syn-depositional relief, which is implied by the elevation of the correlated open lacustrine Pannonian (Tortonian) deposits above the Malé Karpaty Mts. massif and on the Danube Basin margin. The depositional history of the Lake Pannon transgression was soon followed (~ 1 Ma) by the regression of the paleo-Danube deltaic depositional system, and this has also been observed on other pre-Cenozoic blocks across the basin system, such as the Transdanubian Range and Mecsek Mts. The settings could be explained by the loading-induced subsidence of the prograding shelf-slope.

The application of authigenic $^{10}\text{Be}/^9\text{Be}$ dating brought another piece of evidence that in the case of high input of terrestrial material into lacustrine environment close to river deltas, the alluvial initial ratio is more relevant in comparison to the lacustrine one for age calculations; this finding is similar to that documented by Magyar et al. (2019).

Acknowledgements: The geophysical equipment was provided by the Science Park of the Comenius University in Bratislava, and is acknowledged with gratitude. Mária Bielíková, the former Dean of the Faculty of Informatics and Information Technologies of the Slovak Technical University is thanked for her kind agreement to the excavations behind the faculty building. The study was supported financially by the Slovak Research and Development Agency (APVV) under contracts Nos. APVV-15-0575, APVV-16-0121, APVV-16-0146, APVV-20-0120, SK-FR-2015-0017 and SK-AT-2017-0010, and by the Scientific Grant Agency of the Ministry of Education,

Science, Research and Sport of the Slovak Republic and the Slovak Academy of Sciences (VEGA) under the contract No. 2-0122-18. The ASTER AMS national facility (CEREGE, Aix-en-Provence) is supported by the INSU/CNRS, the ANR through the “Projets thématiques d'excellence” program for the “Equipements d'excellence” ASTER-CEREGE action and IRD. Two anonymous reviewers provided very constructive and helpful comments, which significantly improved the overall quality of the manuscript; these, also, are acknowledged with gratitude. Paul Thatcher is thanked for his efforts made during the language correction.

REFERENCES

- Albrecht C., von Rintelen T., Serada S. & Riedel F. (2014) - Evolution of ancient lake bivalves: the Lymnocardiiinae (Cardiidae) of the Caspian Sea. *Hydrobiologia*, 739: 85-94.
- Balázs A., Burov E., Matenco L., Vogt K., Francois T. & Cloetingh S. (2017) - Symmetry during the syn- and post-rift evolution of extensional back-arc basins: The role of inherited orogenic structures. *Earth and Planetary Science Letters*, 462: 86-98.
- Balázs A., Magyar I., Matenco L., Sztanó O., Tóké L. & Horváth F. (2018) - Morphology of a large paleo-lake: Analysis of compaction in the Miocene-Quaternary Pannonian Basin. *Global and Planetary Change*, 171: 134-147.
- Barna P., Starek D. & Pipík R. (2010) - Middle Pannonian Sublittoral ostracod fauna from the locality Sopron (Hungary). *Geologické výzkumy na Moravě a ve Slezsku* 17: 8-9.
- Bartha I.R., Tóké L., Fodor L., Csillag G., Magyar I., Lantos Z. & Sztanó O. (2014) - Deltaic deposits and inundated basement blocks: consequences for paleotopography, Gerecse Hills. In: Bábek O., Grygar T.M. & Uličný, D. (Eds) - Central European Meeting of Sedimentary Geology, Olomouc, Palacky University: 13-14.
- Bartha R., Magyar I., Fodor L., Csillag G., Lantos Z., Tokes L. & Sztanó O. (2015) - Late Miocene lacustrine deltaic deposit: Integrated outcrop and well data from the junction of the Danube Basin and Gerecse Hills, Hungary. 31st IAS Meeting of Sedimentology, Abstract Book, p. 54, doi:10.13140/RG.2.1.5006.9845
- Beidinger A. & Decker K. (2011) - 3D geometry and kinematics of the Lasseer flower structure: Implications for segmentation and seismotectonics of the Vienna Basin strike-slip fault, Austria. *Tectonophysics*, 499: 22-40.
- Bengtson P. (1988) - Open Nomenclature. *Palaeontology* 31: 223-227.
- Benvenuti M. (2003) - Facies analysis and tectonic significance of lacustrine fan-delta successions in the Pliocene-Pleistocene Mugello Basin, Central Italy. *Sedimentary Geology*, 157: 197-234.
- Berka R., Bottig M., Brüstle A.K., Hörfarter C., Schubert G. & Weibold J. (2011) - Base Lower Pannonian model horizon - Pilot Area Vienna Basin. In: Maros, G.A. (Eds) - Summary report of the Geological Models Transenergy Project, TransEnergy - Transboundary Geothermal Energy Resources of Slovenia, Austria, Hungary and Slovakia, pp 189. Available online: <http://transenergy.eu>.

geologie.ac.at/.

- Botka D., Magyar I., Csoma V., Toth E., Šujan M., Rusz-kiczay-Rüdiger Z., Chyba A., Braucher R., Sant K., Coric S., Baranyi V., Bakrac K., Krizmanic K., Bartha I.R., Szabo M. & Silye L. (2019) - Integrated stratigraphy of the Gusterita clay pit: a key section for the early Pannonian (late Miocene) of the Transylvanian Basin (Romania). *Austrian Journal of Earth Sciences*, 112: 221-247.
- Bourbié T., Coussy O. & Zinszner B. (1987) - Acoustics of Porous Media. Gulf Publishing Company, 334 pp.
- Bourlès D., Raisbeck G.M. & Yiou F. (1989) - ^{10}Be and ^9Be in marine sediments and their potential for dating. *Geochimica et Cosmochimica Acta*, 53: 443-452.
- Bown P.R. (1998) - Calcareous Nannofossil Biostratigraphy. British Micropalaeontological Society, Publications Series. Chapman & Hall, London, pp 315.
- Bromley R.G. & Asgaard U. (1991) - Ichnofacies: a mixture of taphofacies and ichnofacies. *Lethaia*, 24: 153-163.
- Budai S., Sebe K., Nagy G., Magyar I. & Sztanó O. (2019) - Interplay of sediment supply and lake-level changes on the margin of an intrabasinal basement high in the Late Miocene Lake Pannon (Mecsek Mts., Hungary). *International Journal of Earth Sciences*, 108: 2001-2019.
- Budai T. & Fodor L. (eds) (2008) - Geology of the Vértes Hills. Explanatory Book to the Geological Map of the Vértes Hills (1:50,000). Geological Institute of Hungary, Budapest, 368 pp.
- Carcaillet J., Bourles D.L., Thouveny N. & Arnold M. (2004) - A high resolution authigenic $^{10}\text{Be}/^9\text{Be}$ record of geomagnetic moment variations over the last 300 ka from sedimentary cores of the Portuguese margin. *Earth and Planetary Science Letters*, 219: 397-412.
- Cartigny M.J.B., Eggenhuisen J.T., Hansen E.W.M. & Postma G. (2013) - Concentration-dependent flow stratification in experimental high-density turbidity currents and their relevance to turbidite facies models. *Journal of Sedimentary Research*, 83: 1046-1064.
- Ćorić S. (2006) - Middle/Upper Miocene (Sarmatian/Pannonian) endemical calcareous nannoplankton from the Central Paratethys. Paper presented at the 11th International Nannoplankton Association Conference, Lincoln, Nebraska, Program with abstracts: 32-34.
- Csillag G., Sztanó O., Magyar I. & Hámori Z. (2010) - Stratigraphy of the Kálla Gravel in Tapolca Basin based on multi-electrode probing and well data. *Földtani Közlemény*, 140: 183-196.
- Cziczér I., Magyar I., Pipik R., Böhme M., Ćorić S., Bakrač K., Sütő-Szentai M., Lantos M., Babinszki E. & Müller P. (2009) - Life in the sublittoral zone of long-lived Lake Pannon: Paleontological analysis of the Upper Miocene Szák Formation, Hungary. *International Journal of Earth Sciences*, 98: 1741-1766.
- Dumas S. & Arnott R.W.C. (2006) - Origin of hummocky and swaley cross-stratification - The controlling influence of unidirectional current strength and aggradation rate. *Geology*, 34: 1073-1076.
- Fordinál K. (1995) - Bivalvia (Dreissenidae, Cardiidae) from the Upper Miocene sediments in Bratislava. *Geologické práce, Správy*, 100: 27-36.
- Fordinál K. (1997) - Mollusc (Gastropoda, Bivalvia) from the Pannonian deposits of western part of Danube Basin (Pezinok claypit). *Slovak Geological Magazine*, 3: 263-283.
- Fordinál K. & Harčová E. (1997) - Izotopové zloženie O a C vo vápniťých schránkach panónskych mäkkýšov z územia Bratislavy - indikátor paleoekologických pomerov. *Mineralia Slovaca*, 29: 50-60.
- Fordinál K. & Tuba L. (1992) - Biostratigrafické a paleoekologické vyhodnotenie sedimentov územia centrálnej časti Bratislavy. *Geologické práce, Správy*, 96: 63-68.
- Fuchs T. (1870) - Die Fauna der Congerenschichten von Radmanest im Banate. *Jahrbuch der k.k. geologischen Reichsanstalt*, 20: 343-364.
- Galović I. (2017) - Sarmatian calcareous nannofossil assemblages in the SW Paratethyan marginal marine environments: Implications for palaeoceanography and the palaeoclimate. *Progress in Oceanography*, 156: 209-220.
- García-García F., Fernández J., Visceras C. & Soria J.M. (2006) - Architecture and sedimentary facies evolution in a delta stack controlled by fault growth (Betic Cordillera, southern Spain, late Tortonian). *Sedimentary Geology*, 185: 79-92.
- Geological map of Slovakia 1:50,000 [online]. Bratislava, State geological institute of Dionýz Štúr. Available online on: <http://apl.geology.sk/gm50js>. Accessed 2020-05-10.
- Ghinassi M. (2007) - The effects of differential subsidence and coastal topography on high-order transgressive-regressive cycles: Pliocene nearshore deposits of the Val d'Orcia Basin, Northern Apennines, Italy. *Sedimentary Geology*, 202: 677-701.
- Gingras M.K., MacEachern J.A., Dashtgard S.E., Zonneveld J.-P., Schoengt J., Ranger M.J. & Pemberton S.G. (2012) - Estuaries In: Knaust D. & Bromley E.G. (Eds) - Trace Fossils as Indicators of Sedimentary Environments. *Developments in Sedimentology*, 64: 463-505.
- Gross M., Piller W.E., Scholger R. & Gitter F. (2011) - Biotic and abiotic response to palaeoenvironmental changes at Lake Pannons' western margin (Central Europe, Late Miocene). *Palaeogeography, Palaeoclimatology, Palaeoecology*, 312: 181-193.
- Gvirtzman Z. (2001) - Lateral thickening of sedimentary units: Sediment compaction vs. Tectonics. *Tectonophysics*, 340: 109-115.
- Harzhauser M., Daxner-Hock G. & Piller E.W. (2004) - An integrated stratigraphy of the Pannonian (Late Miocene) in the Vienna Basin. *Austrian Journal of Earth Sciences*, 95-96: 6-19.
- Harzhauser M., Kovar-Eder J., Nehyba S., Strobitzher-Hermann M., Schwarz J., Wojcicki J. & Zorn I. (2003) - An Early Pannonian (Late Miocene) transgression in the Northern Vienna Basin. The paleoecological feedback. *Geologica Carpathica*, 54: 41-52.
- Harzhauser M., Kowalke T. & Mandic O. (2002) - Late Miocene (Pannonian) Gastropods of Lake Pannon with Special Emphasis on Early Ontogenetic Development. *Annalen des naturhistorischen Museums in Wien*, 103A: 75-141.

- Harzhauser M. & Mandic O. (2008) - The muddy bottom of Lake Pannon - a challenge for dreissenid settlement (Late Miocene; Bivalvia). *Palaeogeography, Palaeoclimatology, Palaeoecology*, 204: 331-352.
- Harzhauser M. & Mandic O. (2008) - Neogene lake systems of Central and South-Eastern Europe: Faunal diversity, gradients and interrelations. *Palaeogeography, Palaeoclimatology, Palaeoecology*, 260: 417-434.
- Harzhauser M. & Mandic O. (2010) - Neogene dreissenids in Central Europe: evolutionary shifts and diversity changes. In: van der Velde G., Rajagopal S. & bij de Vaate A. (Eds) - *The Zebra Mussel in Europe*: 11-28. Backhuys Publisher, Leiden.
- Harzhauser M., Mandic O., Kranner M., Lukeneder P., Kern A.K., Gross M., Carnevale G. & Jawecki C. (2018) - The Sarmatian/Pannonian boundary at the western margin of the Vienna Basin (City of Vienna, Austria). *Austrian Journal of Earth Sciences*, 111: 26-47.
- Harzhauser M. & Tempfer P.M. (2004) - Late Pannonian wetland ecology of the Vienna Basin based on molluscs and lower vertebrate assemblages (Late Miocene, MN 9, Austria). *Courier Forschungsinstitut Senckenberg*, 246: 55-68.
- Helland-Hansen W. & Hampson G.J. (2009) - Trajectory analysis: Concepts and applications. *Basin Research*, 21: 454-483.
- Hilgen F.J., Lourens L.J. & Van Dam J.A., (2012) - The Neogene period. In: Gradstein F.M., Ogg J.G., Schmitz M.D. & Ogg G. (Eds) - *A Geologic Time Scale 2012*: 923-978. Elsevier, Amsterdam.
- Hók J., Šujan M. & Šípka F. (2014) - Tectonic division of the Western Carpathians: An overview and a new approach. *Acta Geologica Slovaca*, 6: 135-143.
- Hölzel M., Wagreich M., Faber R. & Strauss P. (2008) - Regional subsidence analysis in the Vienna Basin (Austria). *Austrian Journal of Earth Sciences*, 101: 88-98.
- Hörnes M. (1862) - Die fossilen Mollusken des Tertiär-Beckens von Wien. II. Bivalven. *Abhandlungen der Geologischen Reichsanstalt*, 2: 117-214.
- Horusitzky H. (1907) - Die agrogeologischen Verhältnisse des südlichen Teiles der Kleinen Karpathen. *Jahresbericht der Königlich Ungarischen Geologischen Reichsanstalt (Budapest)*: 141-167.
- Horváth F., Bada G., Szafián P., Tari G., Ádám A. & Cloetingh S. (2006) - Formation and deformation of the Pannonian Basin: Constraints from observational data. In: Gee D.G. & Stephenson R.A. (Eds) - *European Lithosphere Dynamics*. *Geological Society, London, Memoirs*, 32: 191-206.
- Hyžný M., Šimo V. & Starek D. (2015) - Ghost shrimps (Decapoda: Axiidea: Callianassidae) as producers of an Upper Miocene trace fossil association from sublittoral deposits of Lake Pannon (Vienna Basin, Slovakia). *Palaeogeography, Palaeoclimatology, Palaeoecology*, 425: 50-66.
- Chmeleff J., von Blanckenburg F., Kossert K. & Jakob D. (2010) - Determination of the Be-10 half-life by multicollector ICP-MS and liquid scintillation counting. *Nuclear Instruments and Methods in Physics Research B*, 268: 192-199.
- Jelínek J., Staněk F., Vizi L. & Honěk J. (2011) - Evolution of lignite seams within the South Moravian Lignite Coalfield based on certain qualitative data. *International Journal of Coal Geology*, 87: 237-252.
- Jiríček R. (1985) - Die Ostracoden des Pannonien. In: Papp A. (Ed.) - *Chronostratigraphie und Neostatotypen, Miozän der Zentral Paratethys, Bd. VII, M6 Pannonien (Slavonien und Serbien)*. Akadémiai Kiado, Budapest, pp. 378-408.
- Joniak P., Šujan M., Fordinál K., Braucher R., Rybár S., Kováčová M., Kováč M., Aumaitre G., Bourlès D.L. & Keddadouche K. (2020) - The age and paleoenvironment of a late Miocene floodplain alongside Lake Pannon: Rodent and mollusk biostratigraphy coupled with authigenic ¹⁰Be/⁹Be dating in the northern Danube Basin of Slovakia. *Palaeogeography, Palaeoclimatology, Palaeoecology*, 538: 109482.
- Kaesler R.L., Kontrovitz M. & Taunton S. (1993) - Crushing strength of *Puriana pacifica* (Ostracoda), an experimental approach to taphonomy. *Journal of Paleontology*, 67: 1005-1010.
- Karpytchev M., Ballu V., Krien Y., Becker M., Goodbred S., Spada G., Calmant S., Shum C.K. & Khan Z. (2018) - Contributions of a Strengthened Early Holocene Monsoon and Sediment Loading to Present-Day Subsidence of the Ganges-Brahmaputra Delta. *Geophysical Research Letters*, 45: 1433-1442.
- Knaust D. (2017) - *Atlas of Trace Fossils in Well Core: Appearance, Taxonomy and Interpretation* (Springer, New York), 209 pp.
- Kontrovitz M. (1967) - An investigation of ostracode preservation. *Quarterly Journal of the Florida Academy of Sciences*, 29: 171-177.
- Korschinek G., Bergmaier A., Faestermann T., Gerstmann U.C., Knie K., Rugel G., Wallner A., Dillmann I., Dollinger G., von Gostomski C.L., Kossert K., Maiti M., Poutivtsev M. & Remmert A. (2010) - A new value for the half-life of Be-10 by Heavy-Ion Elastic Recoil Detection and liquid scintillation counting. *Nuclear Instruments and Methods in Physics Research B*, 268: 187-191.
- Kostic B., Becht A. & Aigner T. (2005) - 3-D sedimentary architecture of a Quaternary gravel delta (SW-Germany): Implications for hydrostratigraphy. *Sedimentary Geology*, 181: 147-171.
- Kováč M., Baráth I., Fordinál K., Grigorovich A.S., Halásová E., Hudáčková N., Joniak P., Sabol M., Slamková M., Šliwa I. & Vojtko R. (2006) - Late Miocene to Early Pliocene sedimentary environments and climatic changes in the Alpine-Carpathian-Pannonian junction area: A case study from the Danube Basin northern margin (Slovakia). *Palaeogeography, Palaeoclimatology, Palaeoecology*, 238: 32-52.
- Kováč M., Baráth I., Kováčová-Slamková M., Pipík R., Hlavatý I. & Hudáčková N. (1998) - Late Miocene paleoenvironments and sequence stratigraphy: Northern Vienna Basin. *Geologica Carpathica*, 49: 445-458.
- Kováč M., Márton E., Oszczytko N., Vojtko R., Hók J., Králiková S., Plašienka D., Klučiar T., Hudáčková N. & Oszczytko-Clowes M. (2017) - Neogene palaeogeog-

- raphy and basin evolution of the Western Carpathians, Northern Pannonian domain and adjoining areas. *Global and Planetary Change*, 155: 133-154.
- Kováč M., Synak R., Fordinál K., Joniak P., Tóth C., Vojtko R., Nagy A., Baráth I., Maglay J. & Minár J. (2011) - Late Miocene and Pliocene history of the Danube Basin: Inferred from development of depositional systems and timing of sedimentary facies changes. *Geologica Carpathica*, 62: 519-534.
- Kovács Á., Sebe K., Magyar I., Szurominé K.A. & Kovács E. (2018) - Upper miocene sedimentation and tectonics in the northern imbricate zone (Eastern Mecsek Mts, SW Hungary). *Földtani Közlöny*, 148: 327-340.
- Lebatard A.E., Bourlès D.L., Düringer P., Jolivet M., Braucher R., Carcaillet J., Schuster M., Arnaud N., Monié P., Lhoreau F., Likius A., Mackaye H.T., Vignaud P. & Brunet M. (2008) - Cosmogenic nuclide dating of Sahelanthropus tchadensis and Australopithecus bahrelghazali: Mio-Pliocene hominids from Chad. *Proceedings of the National Academy of Sciences of the United States of America*, 105: 3226-3231.
- Lee E.Y. & Wägreich M. (2017) - Polyphase tectonic subsidence evolution of the Vienna Basin inferred from quantitative subsidence analysis of the northern and central parts. *International Journal of Earth Sciences*, 106: 687-705.
- Leaman M., McIlroy D. & Herringshaw L.G. (2015) - What does Ophiomorpha irregulaire really look like? *Palaeogeography Palaeoclimatology Palaeoecology* 439: 38-49.
- Lenhardt W.A., Švancara J., Melichar P., Pazdírková J., Havíř J. & Sýkorová Z. (2007) - Seismic activity of the Alpine-Carpathian-Bohemian Massif region with regard to geological and potential field data. *Geologica Carpathica*, 58: 397-412.
- Li Z., Bhattacharya J. & Schieber J. (2015) - Evaluating along-strike variation using thin-bedded facies analysis, Upper Cretaceous ferronotom delta, Utah. *Sedimentology*, 62: 2060-2089.
- Lyul'eva S.A. (1989) - New Miocene and Pliocene calcareous nannofossils of the Ukraine. *Dopovidi Akad Nauk Ukrainskoi RSR Ser B - Geol Khim ta Bioi Nauki*, 1: 10-14.
- Magyar I., Cziczter I., Sztanó O., Dávid Á. & Johnson G. (2016) - Palaeobiology, palaeoecology and stratigraphic significance of the Late Miocene cockle *Lymnocardium soproniense* from Lake Pannon. *Geologica Carpathica*, 67: 561-571.
- Magyar I., Geary D.H. & Müller P. (1999) - Paleogeographic evolution of the Late Miocene Lake Pannon in Central Europe. *Palaeogeography, Palaeoclimatology, Palaeoecology*, 147: 151-167.
- Magyar I., Lantos M., Ujszaszi K. & Kordos L. (2007) - Magnetostratigraphic, seismic and biostratigraphic correlations of the Upper Miocene sediments in the north-western Pannonian Basin System. *Geologica Carpathica*, 58: 277-290.
- Magyar I., Müller P., Geary D.H., Sanders H.C. & Tari G. (1999) - Diachronous deposits of Lake Pannon in the Kisalföld Basin reflect basin and mollusc evolution. *Abhandlungen der Geologischen Bundesanstalt Wien*, 56: 669-678.
- Magyar I., Radivojevic D., Sztano O., Synak R., Ujszaszi K. & Pocsik M. (2013) - Progradation of the paleo-Danube shelf margin across the Pannonian Basin during the Late Miocene and Early Pliocene. *Global and Planetary Change*, 103: 168-173.
- Magyar I., Sztanó O., Sebe K., Katona L., Csoma V., Görög Á., Tóth E., Szuromi-Korecz A., Šujan M., Braucher R., Ruszkiczay-Rüdiger Z., Koroknai B., Wórum G., Sant K., Kelder N. & Krijgsman W. (2019) - Towards a high-resolution chronostratigraphy and geochronology for the Pannonian stage: Significance of the Paks cores (central Pannonian basin). *Földtani Közlöny*, 149: 351-370.
- Marko F. & Jureňa V. (1999) - Zlomová tektonika východného okraja viedenskej panvy a hrastu Malých Karpát. *Mineralia Slovaca*, 31: 513-524.
- Martini E. (1971) - Standard Tertiary and Quaternary calcareous nannoplankton zonation. In: Farinacci A. (Ed.) - Proceedings of the Second Planktonic Conference Roma 1970, Edizioni Tecnoscienza, Rome: 739-785.
- Merchel S. & Herpers U. (1999) - An update on radiochemical separation techniques for the determination of long-lived radionuclides via accelerator mass spectrometry. *Radiochimica Acta*, 84: 215-219.
- Meisch C. (2000) - Freshwater Ostracoda of Western and Central Europe. In: Schwoerbel J. & Zwick P. (Eds) - Süßwasserfauna von Mitteleuropa 8/3, Spektrum Akademischer Verlag, Heidelberg, 522 pp.
- Meszaros L.G. (2000) - New results for the Late Miocene Soricidae stratigraphy in the Pannonian Basin. *Newsletters on Stratigraphy*, 38: 1-11.
- Nagy A., Fordinál K., Brzobohatý R., Uher P. & Raková J. (1995) - Vrchný Miocén juhovýchodného okraja Malých Karpát (vrt Ma-1, Bratislava). *Mineralia Slovaca*, 27: 113-132 (in Slovak with English abstract).
- Nemčok A., Mahr T., Malgot J., Vámoš F. & Točík K. (1966) - Bratislava - Mlynská dolina - vysokoškolský areál, výstavba inžinierskych sietí, II. etapa, VP, IGP. Katedra geotechniky Stavebnej fakulty SVŠT. Manuscript, Geofond Nr. 16702, pp 38 Available online on <https://da.geology.sk/navigator/?desktop=Public>.
- Oertli H.J. (1971) - The aspect of Ostracode faunas - a possible new tool in petroleum sedimentology. In: Oertli H.J. (Ed.) - Paléocologie des Ostracodes. *Bulletin Centre de Recherches Pau-SNPA*, suppl. 5: 137-151.
- Papp A. (1950) - Übergangsformen von Congeria zu Dreissenia aus dem Pannon des Wiener Beckens. *Annalen des Naturhistorischen Museums Wien*, 57: 148-156.
- Papp A. (1951) - Das Pannon des Wiener Beckens. *Mitteilungen der Geologischen Gesellschaft in Wien*, 39-41: 99-193.
- Papp A., Jámbo A. & Steininger F.E. (Eds) (1985) - M6 Pannonien (Slavonien und Serbien). *Chronostratigraphie und Neostratotypen*, 7: 1-636.
- Patruno S. & Helland-Hansen W. (2018) - Clinofolds and clinofold systems: Review and dynamic classification scheme for shorelines, subaqueous deltas, shelf edges and continental margins. *Earth-Science Reviews*, 185: 202-233.
- Paulissen W., Luthi S., Grunert P., Čorić S. & Harzhauser M. (2011) - Integrated high-resolution stratigraphy of a

- Middle to Late Miocene sedimentary sequence in the central part of the Vienna Basin. *Geologica Carpathica*, 62: 155-169.
- Paulissen W.E. & Luthi S.M. (2011) - High-frequency cyclicity in a Miocene sequence of the Vienna Basin established from high-resolution logs and robust chronostratigraphic tuning. *Palaeogeography, Palaeoclimatology, Palaeoecology*, 307: 313-323.
- Pemberton S.G., MacEachern J.A., Dashtgard S.E., Bann K.L., Gingras M.K. & Zonneveld J.P. (2012) - Shorefaces. In: Knaust D., Bromley E.G. (Eds) - Trace Fossils as Indicators of Sedimentary Environments. *Developments in Sedimentology* 64: 563-603.
- Pipík R. (1998) - Salinity changes recorded by ostracoda assemblages found in Pannonian sediments in the western margin of the Danube Basin. *Bulletin des centres de recherches exploration-production Elf-Aquitaine, Pau, Mémoires*, 20: 167-177.
- Pipík R., Bodergat A.-M., Briot D., Kováč M., Kráľ J., Zielinski G. (2012) - Physical and biological properties of the Late Miocene, long-lived Turiec Basin Western Carpathians (Slovakia) and its paleobiotopes. *Journal of Paleolimnology*, 47: 233-249.
- Pipík R., Minati K., Buttinger R., Gross M. & Knobloch J. (2007) - Ecological radiation of Cyprideis in the Late Miocene Lake Pannon. European Ostracodologist's Meeting VI - Abstract Volume, Frankfurt am Main, pp 28.
- Pipík R., Starek D., Seko M. & Sýkorová M. (2013) - Ostracods of the Late Miocene long lived Lake Pannon. Abstract book of 17th International Symposium on Ostracoda, Rome 2013. *Il Naturalista Siciliano* 37: 291-294.
- Polák M., Plašienka D., Kohút M., Putiš M., Bezák V., Filo I., Olšavský M., Havrila M., Buček S., Maglay J., Elečko M., Fordinál K., Nagy A., Hraško L., Németh Z., Ivanička J. & Broska I. (2011) - Geological map of the Malé Karpaty Mts. in scale 1 : 50,000. Ministry of environment of the Slovak Republic and State Geological Survey of Dionýz Štúr, Bratislava.
- Polák M., Plašienka D., Kohút M., Putiš M., Bezák V., Maglay J., Olšavský M., Filo I., Havrila M., Buček S., Elečko M., Fordinál K., Nagy A., Hraško L., Németh Z., Malík P., Liščák P., Madarás J., Slavkay M., Kubeš P., Kucharič L., Boorová D., Zlinská A., Siráňová Z. & Žecová K. (2012) - Explanatory notes to the geological map of the Malé Karpaty Mts. in scale 1 : 50,000. State Geological Survey of Dionýz Štúr, Bratislava, 287 pp.
- Radionova E.P., Golovina L.A., Filippova N.Y., Trubikhin V.M., Popov S.V., Goncharova I.A., Vernigorova Y.V. & Pinchuk T.N. (2012) - Middle-Upper Miocene stratigraphy of the Taman Peninsula, Eastern Paratethys. *Central European Journal of Geosciences*, 4: 188-204.
- Reischenbacher D., Refelj H., Sachsenhofer R.F., Jelen B., Čorić S., Gross M. & Reichenbacher B. (2007) - Early Badenian paleoenvironment in the Lavanttal Basin (Mühldorf Formation; Austria): Evidence from geochemistry and paleontology. *Austrian Journal of Earth Sciences*, 100: 202-229.
- Reynolds J.M. (1997) - An Introduction to Applied and Environmental Geophysics. John Wiley and Sons Ltd, Chichester, 796 pp.
- Rögl F., Zapfe H., Bernor L., Brzobohatý R., Daxner-Höck G., Draxler I., Fejfar O., Faudant J., Herrmann P., Rabeder G., Schultz P. & Zetter R. (1993) - Die Primatenfundstelle Götzendorf an der Leitha (Obermiozän des Wiener Beckens, Nieder-Österreich). *Jahrbuch der Geologischen Bundesanstalt*. 136: 503-526.
- Rohais S., Eschard R. & Guillocheau F. (2008) - Depositional model and stratigraphic architecture of rift climax Gilbert-type fan deltas (Gulf of Corinth, Greece). *Sedimentary Geology*, 210: 132-145.
- Rossi V.M., Perillo M.M., Steel R.J. & Olariu C. (2017) - Quantifying mixed-process variability in shallow-marine depositional systems: What are sedimentary structures really telling us? *Journal of Sedimentary Research*, 87: 1060-1074.
- Sandmeier K.J. (2016) - Reflexw - GPR and seismic processing software. Sandmeier geophysical research 2017. Available on: <http://www.sandmeier-geo.de/reflexw.html>. <http://www.sandmeier-geo.de/reflexw.html>. Accessed 2018-01-04.
- Sebe K., Magyar I., Kovačić M., Sztanó O., Botka D., Csoma V., Korecz A., Krizmanić K. & Kovács Á. (2019) - Lake Pannon calcareous marls in the SW Pannonian Basin: lithology, stratigraphy and bounding surfaces. AAPG Europe Regional Conference - Paratethys Petroleum System Between Central Europe and the Caspian Region, Vienna, 50 pp.
- Schultz O. (2003) - Bivalvia neogenica (Lucinoidea-Mactroidea). In: Piller W.E. (Ed) - *Catalogus Fossilium Austriae*, Band 1/Teil 2. Verlag der Österreichischen Akademie der Wissenschaften, Wien, pp I-X and 381-690.
- Sheehan J.R., Doll W.E. & Mandell W.A. (2005) - An Evaluation of Methods and Available Software for Seismic Refraction Tomography Analysis. *Journal of Environmental and Engineering Geophysics*, 10: 21-34.
- Simon Q., Ledru M.P., Sawakuchi A.O., Favier C., Mineli T.D., Grohmann C.H., Guedes M., Bard E., Thouveny N., Garcia M., Tachikawa K. & Rodríguez-Zorro P.A. (2020) - Chronostratigraphy of a 1.5±0.1 Ma composite sedimentary record from Colônia basin (SE Brazil): Bayesian modeling based on paleomagnetic, authigenic ¹⁰Be/⁹Be, radiocarbon and luminescence dating. *Quaternary Geochronology*, 58: 101081.
- Simon Q., Thouveny N., Bourlès D.L., Nuttin L., Hillaire-Marcel C. & St-Onge G. (2016) - Authigenic ¹⁰Be/⁹Be ratios and ¹⁰Be-fluxes (²³⁰Th_{xs}-normalized) in central Baffin Bay sediments during the last glacial cycle: Paleoenvironmental implications. *Quaternary Science Reviews*, 140: 142-162.
- Spencer C.J., Yakymchuk C. & Ghaznavi M. (2017) - Visualising data distributions with kernel density estimation and reduced chi-squared statistics. *Geoscience Frontiers*, 8: 1247-1252.
- Stow D.A. (2005) - Sedimentary Rocks in the Field. A Colour Guide. Manson Publishing, London, 320 pp.
- Sztanó O., Kováč M., Magyar I., Šujan M., Fodor L., Uhrin A.,

- Rybár S., Csillag G. & Tokés L. (2016) - Late Miocene sedimentary record of the Danube/Kisalföld Basin: Interregional correlation of depositional systems, stratigraphy and structural evolution. *Geologica Carpathica*, 67: 525-542.
- Szتانó O., Magyar I., Szónoky M., Lantos M., Müller P., Lenkey L., Katona L. & Csillag G. (2013) - Tihany Formation in the surroundings of Lake Balaton: Type locality, depositional setting and stratigraphy. *Földtani Közlemények*, 143: 73-98.
- Szتانó O., Sebe K., Csillag G. & Magyar I. (2015) - Turbidites as indicators of paleotopography, Upper Miocene Lake Pannon, Western Mecsek Mountains (Hungary). *Geologica Carpathica*, 66: 331-344.
- Šarinová K., Rybár S., Halássová E., Hudáčková N., Jamrich M., Kováčová M. & Šujan M. (2018) - Integrated biostratigraphical, sedimentological and provenance analyses with implications for lithostratigraphic ranking: The Miocene Komjatice depression of the Danube Basin. *Geologica Carpathica*, 69: 382-409.
- Šujan M. (2019) - Bratislava naprieč miliónmi rokov - súhra sedimentácie a tektoniky [Bratislava throughout Millions of Years - Interaction of Sedimentation and Tectonics]. In: Šimkovič V. & Vozárová T. (Eds) - Bratislava a More: 29-42. Spektrum STU, Bratislava.
- Šujan M., Braucher R. & Aster Team (2018a) - A test of reproducible authigenic beryllium extraction from clay sediment in the facility of the Dept. of Geology and Palaeontology, Comenius University in Bratislava (Slovakia). *Acta Geologica Slovaca*, 10: 165-169.
- Šujan M., Braucher R., Kováč M., Boulès D.L., Rybár S., Guillou V. & Hudáčková N. (2016a) - Application of the authigenic $^{10}\text{Be}/^9\text{Be}$ dating method to Late Miocene-Pliocene sequences in the northern Danube Basin (Pannonian Basin System): Confirmation of heterochronous evolution of sedimentary environments. *Global and Planetary Change*, 137: 35-53.
- Šujan M., Braucher R., Rybár S., Maglay J., Nagy A., Fordinál K., Šarinová K., Sýkora M., Józsa Š., AsterTeam and Kováč M. (2018b) - Revealing the late Pliocene to Middle Pleistocene alluvial archive in the confluence of the Western Carpathian and Eastern Alpine rivers: $^{26}\text{Al}/^{10}\text{Be}$ burial dating from the Danube Basin (Slovakia). *Sedimentary Geology*, 377: 131-146.
- Šujan M., Braucher R., Tibenský M., Fordinál K., Rybár S., Kováč M. & AsterTeam (2020) - Effects of spatially variable accommodation rate on channel belt distribution in an alluvial sequence: Authigenic $^{10}\text{Be}/^9\text{Be}$ -based Bayesian age-depth models applied to the upper Miocene Volkovce Fm. (northern Pannonian Basin System, Slovakia). *Sedimentary Geology*, 397: 105566.
- Šujan M., Lačný A., Braucher R., Magdolen P. & Aster Team (2017) - Early Pleistocene age of fluvial sediment in the Stará Garda Cave revealed by $^{26}\text{Al}/^{10}\text{Be}$ burial dating: Implications for geomorphic evolution of the Malé Karpaty Mts. (Western Carpathians). *Acta Carsologica*, 46: 251-264.
- Šujan M., Rybár S., Kováč M., Bielik M., Majcin D., Minár J., Plašienka D., Nováková P. & Kotulová J. (2021) - The polyphase rifting and inversion of the Danube Basin revisited. *Global and Planetary Change*, 196: 103375.
- Šujan M., Slávik I., Galliková Z. & Dovičín P. (2016b) - Pre-Quaternary basement of Bratislava (part 1): Genetic vs. geotechnical characteristics of the Neogene foundation soils. *Acta Geologica Slovaca*, 8: 71-86.
- Tari G. (1994) - Alpine tectonics of the Pannonian Basin. PhD. Thesis, Rice University, Houston, 501 pp.
- Tari G., Horváth F., Rumpler J. & Ziegler P.A. (1992) - Styles of extension in the Pannonian Basin. In: Ziegler P.A. (Ed.) - Geodynamics of Rifting: 203-219. Elsevier, Amsterdam.
- Tonkin N.S. (2012) - Deltas. In: Knaust D. & Bromley E.G. (Eds) - Trace Fossils as Indicators of Sedimentary Environments. *Developments in Sedimentology*, 64: 507-528.
- Uher P., Kohút M., Ondrejka M., Konečný P. & Šiman P. (2014) - Monazite-(Ce) in Hercynian granites and pegmatites of the Bratislava Massif, Western Carpathians: Compositional variations and Th-U-Pb electron-microprobe dating. *Acta Geologica Slovaca*, 6: 215-231.
- Uhrin A. & Szتانó O. (2012) - Water-level changes and their effect on deepwater sand accumulation in a lacustrine system: A case study from the Late Miocene of western Pannonian Basin, Hungary. *International Journal of Earth Sciences*, 101: 1427-1440.
- Vakarelov B.K. & Ainsworth R. (2013) - A hierarchical approach to architectural classification in marginal-marine systems: Bridging the gap between sedimentology and sequence stratigraphy. *AAPG Bulletin*, 97: 1121-1161.
- Vass D. (2002) - Lithostratigrafia Západných Karpát: neogén a budínsky paleogén [EN: Lithostratigraphy of the Western Carpathians: Neogene and Buda Paleogene]. State Geological Survey of Dionýz Štúr, Bratislava, 202 pp.
- Visnovitz F., Horváth F., Surányi G., Magyar Á., Sant K., Csoma V., Šujan M., Braucher R., Magyar I., Szتانó O. & Timár G. (2017) - Results of the TFM-1/13 exploration borehole sampling of Pannonian strata below Lake Balaton. *Földtani Közlemények*, 147: 283-296.
- Willenbring J.K. & von Blanckenburg F. (2010) - Meteoric cosmogenic Beryllium-10 adsorbed to river sediment and soil: Applications for Earth-surface dynamics. *Earth-Science Reviews*, 98: 105-122.
- Yawar Z. & Schieber J. (2017) - On the origin of silt laminae in laminated shales. *Sedimentary Geology*, 360: 22-34.
- Young J.R. (1998) - Neogene In: Bown P.R. (Ed.) - Calcareous Nannofossil Biostratigraphy. British Micropalaeontological Society Publication Series: 225-265.
- Young J.R., Bown P.R. & Lees J.A. (2017) - Nannotax3 website. International Nannoplankton Association. Accessed 21 Apr. 2017. Available online on <http://www.mikrotax.org/Nannotax3>.

